SBL-based Adaptive Sensing Framework for WSN-assisted IoT Applications

Vini Gupta and Swades De

***Abstract*—Wireless sensor networks (WSNs) often have limited battery capacity-sensor nodes which severely limit continuous monitoring based Internet-of-Things (IoT) applications. To substantially increase the lifetime of a densely-deployed WSN for monitoring spatio-temporally varying signal, this paper presents a novel sparse Bayesian learning-based adaptive sensor selection framework. The developed strategy selects an active sensor set and turns off the remaining sensor nodes by jointly optimizing two conflicting performance measures: sensing quality and energy efficiency, while considering prevailing energy parameters of the network. To achieve this, a multi-objective optimization problem is formulated. Further, a joint Principal Component Analysis-Sparse Bayesian Learning (PCA-SBL) scheme is presented which uses PCA-based estimated transformation matrix to sparsify the data sensed by sensors, and subsequently uses approximate overcomplete dictionary-based SBL scheme to estimate it. Employing PCA-SBL based signal estimate, a closed loop adaptive mechanism is developed which estimates variations of the monitored signal to predict the number of active sensors for next measurement cycle such that the sensing error remains within an acceptable range. This predicted value is then used in sensor selection problem to dynamically select the active set. The sensor selection, signal recovery, and feedback loop use spatial and temporal correlation inherent in the monitored phenomenon. Extensive simulation studies validate the energy efficiency and stable sensing performance of the proposed framework using both synthetic and real data of a WSN.**

***Index Terms*—Wireless sensor networks, adaptive sensor selection, multi-objective optimization, sparse Bayesian learning, principal component analysis, network residual energy.**

I. Introduction

With the advent of Internet-of-Things (IoT), wireless sensor networks (WSNs) [1], [2] have become indispensable for numerous applications, such as, environment (air pollution) monitoring [3], industrial process monitoring [4], health-care surveillance [5], and smart cities [6]. However, the battery-constrained sensor nodes (SNs) serve as performance bottleneck since they limit lifespan of such networks. Thus, it becomes mandatory to impart sufficient intelligence at the sensor network level to reduce sensing, transmission, and processing complexity at SNs and prolong their lifespan so as to efficiently realize the concept of IoT.

For densely deployed WSNs monitoring a slowly varying environmental/physical phenomenon, signals measured by SNs often possess temporal and spatial correlations that induce sparsity in them. In fact, this inherent redundancy in signals across the SNs can allow their acquisition using a few SNs without significant data loss. In this way, the inter- and intra-signal correlation can be capitalized to impart intelligence at the data acquisition, representation, and reconstruction levels of WSNs so as to save network energy resource without compromising much on the sensing quality as demonstrated in [7], [8]. Moreover, nowadays to save transmission and processing energy required by the SNs, smart and powerful mobile robot-based central controller is designed wherein the mobile robot collects sampled data by moving to the SNs and delivers it to the central controller which carries out all computationally-intensive processing [9], [10]. Thus, the major tasks left with the sensors is to sense the signal and transmit it to a mobile robot present in its vicinity, when selected by the central entity based on a sensor-selection criterion.

A. Related Works on Sensor Selection

Early works such as [11], [12] proposed to randomly activate a predefined number of SNs. Thereafter, sensor selection criteria which guarantee certain performance measures, such as sensing quality and energy efficiency, have gained substantial research interest. In a greedy approach proposed in [13], the SNs with maximum energy efficiency index γ are selected, where γ is the difference between residual energy and transmission energy of the SN.

Subsequently, several works have been reported in the literature that aim at a guaranteed sensing quality. In a pioneering work [14], the authors proposed a sensor selection strategy which chooses measurements of k out of total m SNs based on a performance measure from experimental design, namely, D-optimality which ultimately minimizes estimation error. Due to NP-hard nature of the optimization problem, the authors therein developed a convex relaxation method to sub-optimally solve it. In [15] it was emphasized further that the optimized sensor selection based sensing matrices offer superior performance compared to those based on random selection. Similarly, the authors in [8] developed D-optimality criterion based iterative sensor selection algorithms for heterogeneous sensing environment considering a Bayesian setting. Further, the work in [16] formulated the sensor selection problem for general non-linear measurement model employing Cramér-Rao lower bound based performance measure.

In a recent extension [17], [18] a fixed number of sensors are selected based on an optimization problem that simultaneously minimize a lower bound on mean squared error (MSE) and maximize the network's energy efficiency. Unlike the above-mentioned works [8], [11]–[14], [16], [17] which exploit only the inherent spatial correlation, the scheme proposed in [18] suggests to exploit the temporal correlation as well by using

V. Gupta and S. De are with the Department of Electrical Engineering and Bharti School of Telecommunications, Indian Institute of Technology Delhi, New Delhi 110016, India (e-mail: vini.gupta@ee.iitd.ac.in; swadesd@ee.iitd.ac.in).

the estimated signal support of previous time instances, as illustrated in work [7].

A more practical and intuitive approach for sensor selection is to adapt sampling rate (i.e., the ratio of number of selected SNs and the total number of SNs) online based on variations of signal being measured [19], [20]; the authors in [21] experimentally validated this intuition. In this context, a sensing, compression, and recovery (SCoRe) framework was developed in [7] for WSNs using combined Principal Component Analysis (PCA) [22] and Compressed Sensing (CS) [23]. Similarly, the authors in [24] proposed an adaptation mechanism which builds a hash table governing the sampling rate for different variations in intensity of the monitored signal such that a desired sensing quality is always achieved.

B. Related Works on Sparse Signal Recovery

A fundamental premise of the adaptive algorithms is the estimate of sensed signal which helps in providing near-accurate feedback about variations of the monitored process to dynamically adapt the sampling rate. Due to the use of limited number of sensor measurements, this inherently sparse sensed signal is recovered in a significantly challenging ill-posed estimation scenario. The works such as [7], [17], [18], [24] employ either Basis Pursuit (BP) [25] or its noisy counterpart: least absolute shrinkage and selection operator (LASSO) [26], for obtaining this critical estimate. Besides this, various relevant state-of-the-art sparse signal recovery techniques that exist in the literature are FOCal Underdetermined System Solver (FOCUSS) [27] and Matching Pursuit (MP) [28]. However, a major limitation with BP [25] and LASSO [26] schemes is that they require fine tuning of a regularization parameter which represent a critical trade-off between the estimation accuracy and the level of sparsity of the underlying unknown signal. Further, the iterative FOCUSS scheme [27] and the greedy MP scheme [28] often yield less sparse solutions [25], [29]. However, the reliable feedback requirement in adaptive algorithms mandates the estimation algorithm to be devoid of convergence errors and user parameters. Towards this end, the sparse Bayesian learning (SBL) framework [29] has been known to exhibit superior sparse signal recovery in various fields such as sparse wireless channel estimation [30], biomedical signal processing [31], target imaging in MIMO radars [32], etc. The SBL framework assigns a parameterized Gaussian prior distribution to unknown weight vector and employs a type-II maximum likelihood criterion to estimate those hyperparameters. Unlike the schemes in [25]–[28], SBL is a user parameter free scheme which provides maximally-sparse solution, free from convergence errors [29].

C. Research Gap and Motivation

The random selection based approaches [11], [12] became obsolete due to their limited achievable performance guarantees as shown in [17]. The greedy selection approach in [13], though guarantees energy efficiency, is often beset by poor estimation performance especially for monitoring applications as shown in [17]. The works such as [8], [14]–[16] surmount the above-mentioned shortcoming by guaranteeing sensing performance. However, these approaches assume a constant residual energy cost associated with the individual sensors which may lead to energy imbalance of nodes. The approaches in [8] are energy-inefficient due to their iterative nature. The works [17], [18] aim to provide both the sensing performance and the energy efficiency to some extent. However, a major limitation of the works in the existing literature is that, they consider a fixed number of measurements based on the implicit assumption of a constant sparsity of the sensed signal, while in reality the sparsity may vary due to spatio-temporal variations of the monitored signal. It is important to adapt the sampling rate with the spatio-temporal dynamics of the to-be-sensed phenomenon. Adaptive sampling rate will also help avoid the possibilities of excessive energy consumption associated with the fixed high-rate sampling and poor sensing performance due to low-rate sampling.

Though the works in [7], [24] consider temporal dynamics of the process to adapt the sampling rate, they leave a few scopes of improvements. Firstly, random sampling employed therein is expected to offer inferior performance. Secondly, the considered same resource cost associated with each SN may result in network residual energy imbalance and hence early outage of network coverage. Thirdly and most importantly, alike TCP congestion window adaptation, exponential increase in sampling rate in [7] may offer good sensing quality but at the cost of degraded energy efficiency. Lastly, the hash table-based mechanism in [24] requires an extensive training which demands data collection at a high sampling rate. Such framework often becomes unviable for joint energy efficiency and sensing quality maximization.

Thus it is observed that, so far none of the work collectively considers process dynamics, sensing quality, and dynamic energy resource of nodes for optimized sensor selection. In fact, a training-free adaptive approach which can better quantify the change in sampling rate to guarantee desired sensing performance with minimal energy cost has not been studied yet. To this end, motivated by higher recovery performance of SBL, this work proposes an SBL-based adaptive sensing framework, to better model the real-world sensing problem in IoT applications.

D. Contributions

Key contributions of this work are as follows.

1) A joint PCA-SBL scheme is described for WSN wherein PCA dynamically learns a transformation matrix that characterizes the correlations inherent to the acquired signal, and thereafter the SBL framework recovers it using an overcomplete dictionary matrix (approximated from the transformation matrix).
2) A multi-objective optimization problem (MOP) for sensor selection is proposed which jointly optimizes a critical trade-off between the estimation performance (sensing quality) and the energy efficiency subject to practical coverage constraints.
3) A novel adaptive sensing framework is developed which predicts the sampling rate for the next measurement cycle based on an estimate of underlying signal's variations

(using its current PCA-SBL estimate). This predicted number is further dynamically updated by the MOP using current energy parameters of SNs while ensuring the required sensing quality.

4) The proposed framework is tested on both real and synthetic data of a WSN. Simulation results clearly illustrate that compared to the state-of-the-art sensing schemes, the proposed adaptive sensing framework provides significant gain in energy saving while maintaining the prescribed sensing quality. Thus, it can serve as a benchmark for realization of diuturnal operations of WSN-assisted IoT applications. Further, the numerical study provides insights on the impact of spatio-temporal dynamics of the monitored process on the duration of WSN operations, which have been missing in the prior art. Superior recovery and reliable feedback guarantees of the SBL over the widely-used sparse recovery scheme, LASSO (basis pursuit denoising), are also demonstrated.

Organization: The layout of the paper is as follows. The data gathering model for WSN is presented in Section II, followed by a description of joint PCA-SBL scheme for sparse signal representation and recovery in Section III. Section IV describes the proposed adaptive sensor selection framework, followed by the simulation results and concluding remarks, respectively in Section V and Section VI.

Notation: In this work, bold lowercase and uppercase letters such as $\mathbf{a}$ and $\mathbf{A}$ denote vectors and matrices respectively. The symbols $\mathbf{0}_{M\times N}$ and $\mathbf{I}_N$ represent a $M \times N$ matrix of zeros and a $N \times N$ identity matrix respectively. For a matrix $\mathbf{A}$, $\mathbf{A}(m,n)$, $A(m,:)$, and $\mathrm{Tr}\{\mathbf{A}\}$ denote the $(m,n)^{th}$ element, m^{th} row, and trace of $\mathbf{A}$ respectively. For a vector $\mathbf{a}$, $a(m)$ and $\|\mathbf{a}\|$ denote the m^{th} element and the standard l_2-norm of $\mathbf{a}$. Throughout the paper, subscript k and superscript (l) refer to the scalar/vector/matrix argument in k^{th} measurement cycle and their estimates in the l^{th} iteration respectively. Further, for matrix $\mathbf{A}$ and vector $\mathbf{a}$, the quantities $\mathbf{A} \in \mathbb{R}^{M\times N}, \mathbf{A} \in \mathbb{S}^N, \mathbf{A} \in \mathbb{S}^N_{++}$, and $\mathbf{a} \in \mathbb{R}^{N\times 1}$ represent a real-valued matrix of size $M\times N$, a symmetric matrix of size $N\times N$, a symmetric positive definite matrix of size $N \times N$, and a real vector of size $N \times 1$ respectively. The operators $(.)^T$, $\mathrm{diag}(\cdot)$, $|.|$, and $\bigcup$ denote the transpose of the vector/matrix, the standard diagonalization operation on a vector, the cardinality, and the set union operation respectively. The set **dom** f represent domain of the function f.

II. System Model for Data Acquisition

Consider a WSN architecture containing densely-deployed battery-powered static sensor nodes which monitor a spatio-temporally varying process, such as air pollution. A central entity, equipped with mobile robot, collects the sensed information from these SNs. Slow spatial variation of the sensed process and dense deployment (spatially proximal SNs) result in spatial correlation among the data sensed by SNs. Unlike the conventional WSNs where all the SNs periodically monitor the underlying process, the aforementioned spatial correlation can be utilized to accurately monitor the process using a subset of SNs while the remaining SNs can sleep. The central controller chooses this subset of SNs, called active set, based on an adaptive sensor selection framework proposed in Section IV. Thereafter, it broadcasts a common signal containing information about the active nodes. Subsequently, a mobile robot collects the sensed data from those active nodes and transmits it to the central entity for reconstructing the process across the entire sensor field. During each cycle, it is assumed that each SN senses the process in a synchronized manner.

Let $\mathbf{z}_k = [z_k(1), \ldots, z_k(N)]^T \in \mathbb{R}^{N\times 1}$ be a spatial signal vector corresponding to pollution signals across N SNs during k^{th} measurement cycle. Let the central entity chooses the active set of nodes $\mathcal{A}_k \subseteq \{1, \ldots, N\}$ for sensing the signal during the k^{th} measurement cycle such that the number of active nodes $M_k = |\mathcal{A}_k| \leq N$. Thus, the sampling rate, defined as ratio of number of active SNs to total number of SNs, is given by $\frac{M_k}{N}$. Since N is fixed, the sampling rate is proportional to M_k. Let $\mathbf{A}_k \in \mathbb{R}^{M_k\times N}$ denote binary sensing matrix which captures the active/sleep status of each SN during the k^{th} measurement cycle. Each row of the sensing matrix $\mathbf{A}_k$ corresponds to one active SN. Thus, if m^{th} row of $\mathbf{A}_k$, $\forall\ 1 \leq m \leq M_k$, represents i^{th} active SN, then $\mathbf{A}_k(m,:) = [\mathbf{A}_k(m,1), \ldots, \mathbf{A}_k(m,N)] \in \mathbb{R}^{1\times N}$ is given by,

$$\mathbf{A}_k(m,n) = \begin{cases} 1 & , n = i \ \text{ s.t. } i \in \mathcal{A}_k \\ 0 & , n \in \{1,\ldots,N\} \setminus \{i\}. \end{cases} \tag{1}$$

Thus, as in [8], [17], data gathering model is given by,

$$\widetilde{\mathbf{y}}_k = \mathbf{A}_k\mathbf{z}_k + \mathbf{n}_k, \tag{2}$$

where $\widetilde{\mathbf{y}}_k \in \mathbb{R}^{M_k\times 1}$ denotes measurement vector containing measured signals collected from SNs belonging to the active set $\mathcal{A}_k$ and $\mathbf{n}_k \in \mathbb{R}^{M_k\times 1}$ is the additive white Gaussian noise vector with independent and identically distributed (IID) components having zero mean and variance σ^2. The noise vector $\mathbf{n}_k$ combines both measurement and transmission noises, and is independent of the sensing matrix $\mathbf{A}_k$ and the signal vector $\mathbf{z}_k$ corresponding to the monitored process.

III. Joint PCA-SBL Scheme for Sparse Signal Representation and Recovery

The above monitoring scenario is ill-posed as the true pollution signal vector across all SNs ($\mathbf{z}_k$) is to be estimated at the central controller using the pollution signal measured by a few active SNs ($\widetilde{\mathbf{y}}_k$). However, the spatial correlation among components of the signal vector $\mathbf{z}_k$ induces sparsity which allows its reconstruction in some transformed domain using under-sampled measured data [23]. Thus, the signal vector $\mathbf{z}_k$ can be represented as a sparse vector $\mathbf{x}_k \in \mathbb{R}^{N\times 1}$ under some sparsifying matrix $\mathbf{B}_k \in \mathbb{R}^{N\times N}$ and estimated using a sparse signal recovery technique as outlined in the subsections below.

A. PCA-based Sparse Signal Representation

In the existing literature [33], different sparsification matrices have been used. However, as mentioned in [34], none of them sufficiently sparsify the correlated signal vector $\mathbf{z}_k$. In this work, as in [7], PCA is used for obtaining sparse representation of the vector $\mathbf{z}_k$. PCA [22] is a statistical procedure that

uses an eigenvalue value decomposition of sample covariance matrix to convert a set of correlated observations into a set of uncorrelated ones.

Consider an initial training data set containing K_{tr} instances of the spatial signal vector $\mathbf{z}$ i.e. $\mathcal{T} = \{\mathbf{z}_{k-K_{tr}+1}, \ldots, \mathbf{z}_{k-1}, \mathbf{z}_k\}$. Sample mean vector $\bar{\mathbf{z}}_{\mathcal{T}} \in \mathbb{R}^{N\times 1}$ and sample covariance matrix $\widehat{\mathbf{\Sigma}}_{\mathcal{T}} \in \mathbb{R}^{N\times N}$ are given by,

$$\bar{\mathbf{z}}_{\mathcal{T}} = \frac{1}{|\mathcal{T}|}\sum_{j\in\mathcal{T}} \mathbf{z}_{k-j}, \tag{3}$$

$$\widehat{\mathbf{\Sigma}}_{\mathcal{T}} = \frac{1}{|\mathcal{T}|}\sum_{j\in\mathcal{T}} \left(\mathbf{z}_{k-j} - \bar{\mathbf{z}}_{\mathcal{T}}\right)\left(\mathbf{z}_{k-j} - \bar{\mathbf{z}}_{\mathcal{T}}\right)^T. \tag{4}$$

Let $\mathbf{B}_k \in \mathbb{R}^{N\times N}$ be an orthogonal matrix such that its columns are the orthogonal eigen-vectors of the matrix $\widehat{\mathbf{\Sigma}}_{\mathcal{T}}$ and $\mathbf{\Gamma}_k$ be a diagonal matrix with eigen values of $\widehat{\mathbf{\Sigma}}_{\mathcal{T}}$ as its diagonal elements, i.e. $\widehat{\mathbf{\Sigma}}_{\mathcal{T}} = \mathbf{B}_k\mathbf{\Gamma}_k\mathbf{B}_k^T$. Due to the presence of spatial correlation among components of the signal vector $\mathbf{z}_k, \forall k$ and the temporal correlation among components of the training set $\mathcal{T}$, projection of $\mathbf{z}_k$ onto vector space $\mathcal{R}(\mathbf{B}_k)$ results in a vector $\mathbf{x}_k \in \mathbb{R}^{N\times 1}$ having significant fraction of its energy in a few components. Thus, during any measurement cycle, the vector $\mathbf{x}_k$ is obtained as $\mathbf{x}_k = \mathbf{B}_k^T(\mathbf{z}_k - \bar{\mathbf{z}}_{\mathcal{T}})$ and the resulting sparse representation of the vector $\mathbf{z}_k$ is given by $\mathbf{z}_k = \bar{\mathbf{z}}_{\mathcal{T}} + \mathbf{B}_k\mathbf{x}_k$. The system model (2) becomes,

$$\mathbf{y}_k = \mathbf{\Theta}_k\mathbf{x}_k + \mathbf{n}_k, \tag{5}$$

where $\mathbf{\Theta}_k = \mathbf{A}_k\mathbf{B}_k \in \mathbb{R}^{M_k\times N}$ is estimated equivalent sensing matrix and $\mathbf{y}_k = \widetilde{\mathbf{y}}_k - \mathbf{A}_k\bar{\mathbf{z}}_{\mathcal{T}} \in \mathbb{R}^{M_k\times 1}$ is equivalent measurement vector.

Owing to unavailability of the spatial vector $\mathbf{z}_k$, it is difficult to compute the exact matrix $\mathbf{B}_k$ at the k^{th} measurement cycle. Here, slowly-varying nature of the process monitored by the densely-deployed SNs is exploited, where $\mathbf{B}_k$ is expected to change slowly. Thus, the sparsifying matrix of previous measurement cycle can be used as a coarse estimate of the current sparsifying matrix, i.e. $\mathbf{B}_k \approx \mathbf{B}_{k-1}$. Further, as in [7], [34], this estimate of $\mathbf{B}_k$ is refined online using the initial training set and the previously reconstructed signal vectors $\widehat{\mathbf{z}}_j \ \forall\ j < k$, i.e. $\mathcal{T} = \{\mathbf{z}_{-K_{tr}+1}, \ldots, \mathbf{z}_0, \widehat{\mathbf{z}}_1, \ldots, \widehat{\mathbf{z}}_{k-1}\}$ such that $|\mathcal{T}| = (K_{tr} + k - 1)$. The online refinement of $\mathbf{B}_k$ eliminates the need for rigorous and frequent training of the network and avoids the loss in reconstruction accuracy that would have occurred due to usage of stale estimate of $\mathbf{B}_k$ in recovering the unknown signal vector $\mathbf{z}_k$ (or $\mathbf{x}_k$ in (5)).

B. SBL-based Signal Recovery

This section outlines the sparse Bayesian learning scheme which estimates the unknown vector $\mathbf{x}_k$ using an approximate overcomplete dictionary matrix $\mathbf{\Theta}_k \approx \mathbf{A}_k\mathbf{B}_{k-1}$ and the equivalent measurement vector $\mathbf{y}_k$ during each k^{th} measurement cycle for the signal model (5). This SBL-based estimate is later used to provide a near-accurate feedback to adapt sensor selection algorithm with the varying monitored process.

The SBL framework assumes Gaussian likelihood model for recovery of the monitored phenomenon [29]. During each measurement cycle k, SBL framework [29] assigns a parameterized Gaussian prior to the sparse weight vector $\mathbf{x}_k$ as,

$$p(\mathbf{x}_k;\boldsymbol{\gamma}_k) = \prod_{n=1}^{N}\left(2\pi\gamma_k(n)\right)^{-1/2} e^{-\frac{(x_k(n))^2}{2\gamma_k(n)}}, \tag{6}$$

where $\boldsymbol{\gamma}_k = [\gamma_k(1), \ldots, \gamma_k(N)]^T \in \mathbb{R}^{N\times 1}$ is a hyperparameter vector whose each element $\gamma_k(n)$ corresponds to the variance of element $x_k(n)$ of the weight vector $\mathbf{x}_k$. The Gaussian prior fits well a realistic signal sensed by a WSN. This is due to central limit theorem [35], as the signal $\mathbf{x}_k$, transformed from randomly distributed signal $\mathbf{z}_k$ of WSN, will have Gaussian distribution as $N \to \infty$. Moreover, since the Gaussian prior is a conjugate prior for the Gaussian likelihood function, the closed form expression for posterior density function can be readily obtained. Typically, the hyperparameter vector estimate $\widehat{\boldsymbol{\gamma}}_k$ can be computed following the maximum likelihood estimation procedure [36] wherein the log-likelihood cost function is maximized as follows,

$$\widehat{\boldsymbol{\gamma}}_{k_{ML}} = \arg\max_{\boldsymbol{\gamma}_k \succeq 0}\ \log p(\mathbf{y}_k;\boldsymbol{\gamma}_k). \tag{7}$$

However, due to intractability of the above optimization problem as shown in [29], in this work iterative expectation maximization (EM) algorithm is used to estimate the vector $\boldsymbol{\gamma}_k$ by considering the weight vector $\mathbf{x}_k$ as the latent variable. Let the estimate of hyperparameter vector $\boldsymbol{\gamma}_k$ in l^{th} EM iteration be $\widehat{\boldsymbol{\gamma}}_k^{(l)}$. The E-step in the l^{th} iteration computes expectation of the log-likelihood function as,

$$\begin{aligned}\mathcal{L}\left(\boldsymbol{\gamma}_k \mid \boldsymbol{\gamma}_k^{(l)}\right) &= \mathrm{E}_{\mathbf{x}_k|\mathbf{y}_k;\boldsymbol{\gamma}_k^{(l)}}\left\{\log p(\mathbf{y}_k, \mathbf{x}_k;\boldsymbol{\gamma}_k)\right\} \\ &= \mathrm{E}_{\mathbf{x}_k|\mathbf{y}_k;\boldsymbol{\gamma}_k^{(l)}}\left\{\log p(\mathbf{y}_k \mid \mathbf{x}_k;\boldsymbol{\gamma}_k)\right\} + \\ &\quad \mathrm{E}_{\mathbf{x}_k|\mathbf{y}_k;\boldsymbol{\gamma}_k^{(l)}}\left\{\log p(\mathbf{x}_k;\boldsymbol{\gamma}_k)\right\}.\end{aligned} \tag{8}$$

Here, the posterior distribution of $\mathbf{x}_k$ in the l^{th} iteration is $p\left(\mathbf{x}_k \mid \mathbf{y}_k;\boldsymbol{\gamma}_k^{(l)}\right) \sim \mathcal{N}\left(\boldsymbol{\mu}_{x_k}^{(l)}, \mathbf{\Sigma}_{x_k}^{(l)}\right)$ [29], with *a posteriori* mean vector $\boldsymbol{\mu}_{x_k}^{(l)} \in \mathbb{R}^{N\times 1}$ and covariance matrix $\mathbf{\Sigma}_{x_k}^{(l)} \in \mathbb{R}^{N\times N}$ given by,

$$\boldsymbol{\mu}_{x_k}^{(l)} = \sigma^{-2}\mathbf{\Sigma}_{x_k}^{(l)}\mathbf{\Theta}_k^T\mathbf{y}_k, \tag{9}$$

$$\mathbf{\Sigma}_{x_k}^{(l)} = \left(\sigma^{-2}\mathbf{\Theta}_k^T\mathbf{\Theta}_k + \left(\widehat{\mathbf{\Gamma}}_k^{(l)}\right)^{-1}\right)^{-1}, \tag{10}$$

with $\widehat{\mathbf{\Gamma}}_k^{(l)} = \mathrm{diag}\left(\widehat{\gamma}_k^{(l)}(1), \ldots, \widehat{\gamma}_k^{(l)}(N)\right)$. Employing the matrix inversion lemma [37], the matrix $\mathbf{\Sigma}_{x_k}^{(l)}$ is computed with lesser complexity of $\mathcal{O}\left(M_k^3\right)$ in contrast to the complexity $\mathcal{O}\left(N^3\right)$ associated with the equation (10), as

$$\mathbf{\Sigma}_{x_k}^{(l)} = \widehat{\mathbf{\Gamma}}_k^{(l)} - \widehat{\mathbf{\Gamma}}_k^{(l)}\mathbf{\Theta}_k^T\left(\mathbf{\Sigma}_{y_k}^{(l)}\right)^{-1}\mathbf{\Theta}_k\widehat{\mathbf{\Gamma}}_k^{(l)}, \tag{11}$$

where $\mathbf{\Sigma}_{y_k}^{(l)} = \left(\sigma^2\mathbf{I}_{M_k} + \mathbf{\Theta}_k\widehat{\mathbf{\Gamma}}_k^{(l)}\mathbf{\Theta}^T\right)$. Further, the M-step maximizes $\mathcal{L}\left(\boldsymbol{\gamma}_k \mid \boldsymbol{\gamma}_k^{(l)}\right)$ to obtain the hyperparameter vector

estimate $\widehat{\boldsymbol{\gamma}}_k^{(l+1)}$ as:

$$\begin{aligned}\widehat{\boldsymbol{\gamma}}_k^{(l+1)}(n) &= \arg\max_{\boldsymbol{\gamma}_k(n)} \Big(\mathrm{E}_{\mathbf{x}_k|\mathbf{y}_k;\boldsymbol{\gamma}_k^{(l)}}\left\{\log p\left(\mathbf{y}_k \mid \mathbf{x}_k;\boldsymbol{\gamma}_k\right)\right\}+ \\ &\quad \mathrm{E}_{\mathbf{x}_k|\mathbf{y}_k;\boldsymbol{\gamma}_k^{(l)}}\left\{\log p\left(\mathbf{x}_k;\boldsymbol{\gamma}_k\right)\right\}\Big) \\ &= \boldsymbol{\Sigma}_{x_k}^{(l)}(n,n)+\left(\mu_{x_k}^{(l)}(n)\right)^2. \end{aligned} \tag{12}$$

Finally, after iterating via E- and M-steps for L_{EM} times, the estimate of sparse signal vector is obtained as, $\widehat{\mathbf{x}}_k = \boldsymbol{\mu}_{x_k}^{(L_{EM})}$. At this juncture, it is worth to point out that, by employing SBL-EM framework, as $\widehat{\gamma}_k^{(l)}(n) \rightarrow 0$, the corresponding $\widehat{x}_k^{(l)}(n) \rightarrow 0$, which provides a maximally sparse estimate of the signal vector $\mathbf{x}_k$ without requiring any *a priori* knowledge of its level of sparsity.

IV. Proposed Adaptive Sensing Framework

This section develops the proposed adaptive sensor selection framework that jointly optimizes reconstruction performance and utilization of network remaining energy based on a feedback which is governed by estimated variability of the monitored process.

A. Optimization Problem for Sensor Selection

The proposed sensor selection optimization is run by a central entity to determine an active set $\mathcal{A}_k$ during the k^{th} measurement cycle by optimizing the trade-off between sensing performance and network energy efficiency subject to the practical system constraints. Intuitively, employing measurements from all the SNs to estimate the underlying signal will give the best sensing accuracy, however at an overwhelming expenditure of energy. In contrast, activating a few SNs will save network energy at the cost of information loss due to decreased sensing accuracy. Hence, it is necessary to optimize this crucial node selection trade-off especially when there is redundancy in measurements of closely-spaced SNs.

Let f_1 be the objective function corresponding to error in estimation of the unknown vector $\mathbf{x}_k$ which depends on the error covariance matrix $\boldsymbol{\Sigma}_e = \mathrm{E}\left\{\left(\mathbf{x}_k - \widehat{\mathbf{x}}_k\right)\left(\mathbf{x}_k - \widehat{\mathbf{x}}_k\right)^T\right\} \in \mathbb{R}^{N\times N}$. The sensor selection problem developed herein is based on A-optimality performance measure [14], [38]. Thus, f_1 represents the sum of eigen values of the matrix $\boldsymbol{\Sigma}_e$, i.e. the mean-squared error (MSE) in estimation of the vector $\mathbf{x}_k$ as given by,

$$\begin{aligned} f_1 &= \mathrm{Tr}\left\{\mathrm{E}\left[\left(\mathbf{x}_k - \widehat{\mathbf{x}}_k\right)\left(\mathbf{x}_k - \widehat{\mathbf{x}}_k\right)^T\right]\right\} \\ &= \mathrm{E}\left\{\left\|\mathbf{x}_k - \widehat{\mathbf{x}}_k\right\|^2\right\} = \mathrm{MSE}. \end{aligned} \tag{13}$$

As noted in [17], [18], the performance measure f_1 in (13) depends on the actual estimator and does not have a tractable closed form expression. Moreover, its dependence on the unknown signal vector $\mathbf{x}_k$ makes it unviable for sensor selection problem in practical monitoring scenarios. In this study, this shortcoming is overcome by capitalizing on a theoretical lower bound, namely Bayesian Cramér-Rao bound (BCRB) [36]. The BCRB expression for the PCA-SBL based signal estimation which lower bounds the performance measure f_1 $\left(\text{i.e. } \mathrm{E}\left\{\left\|\mathbf{x}_k - \widehat{\mathbf{x}}_k\right\|^2\right\} \geq \mathrm{BCRB}\right)$ is given in (14), with detailed derivation outlined in appendix A,

$$\mathrm{BCRB} = \mathrm{Tr}\left\{\left(\frac{1}{\sigma^2}\mathbf{B}_k^T\mathbf{A}_k^T\mathbf{A}_k\mathbf{B}_k + \boldsymbol{\Gamma}_k^{-1}\right)^{-1}\right\}. \tag{14}$$

Minimizing BCRB provides minimum achievable MSE performance of a benchmark estimator under scenarios with large number of measurements and $\sigma^2 \rightarrow 0$. Thus, minimizing BCRB minimizes MSE, as shown in [16], [17]. Choice of using BRCB stems from the fact that the SBL framework assigns a parameterized Gaussian prior to the unknown signal vector $\mathbf{x}_k$ and the BCRB too considers the prior distribution of the vector $\mathbf{x}_k$. Note that, knowledge of the prior associated with the unknown vector $\mathbf{x}_k$ can be obtained form previous measurements [16], [36]. Besides this, BCRB is independent of the unknown signal vector $\mathbf{x}_k$ and even does not demand availability of actual measurements $\widetilde{\mathbf{y}}_k$ of sensor nodes. This has significant practical relevance as it enables the sensor selection before the data acquisition. Most importantly, this fundamental performance bound has a very appealing structure which facilitates in posing the sensor selection problem as a sensing matrix design problem. To see this, let $\widetilde{\mathbf{A}}_k$ be a diagonal matrix defined as $\widetilde{\mathbf{A}}_k = \mathbf{A}_k^T\mathbf{A}_k \in \mathbb{R}^{N\times N}$ such that its structure is given by,

$$\widetilde{\mathbf{A}}_k(n,n) = \begin{cases} 1 & ,\ n \in \mathcal{A}_k \\ 0 & ,\ n \notin \mathcal{A}_k. \end{cases} \tag{15}$$

The matrix $\widetilde{\mathbf{A}}_k$ can be represented using row permutation operation as, $\widetilde{\mathbf{A}}_k = \boldsymbol{\Pi}\begin{bmatrix}\mathbf{A}_k \\ \mathbf{0}_{(N-M_k)\times N}\end{bmatrix}$ [18] where $\boldsymbol{\Pi}$ and $\mathbf{0}_{(N-M_k)\times N}$ denote row permutation matrix and a matrix of $(N-M_k)$ rows of N zero elements each respectively. Each diagonal element $\widetilde{\mathbf{A}}_k(n,n) = 1$ corresponds to the n^{th} active SN. Thus, the BCRB-based sensor selection problem can be equivalently viewed as sensing matrix design problem. Further, the matrix $\mathbf{B}_k$ in (14) characterizes the spatial and temporal correlations of the monitoring process. The objective function (14) is a convex function with detailed derivation of proof of convexity given in appendix B.

Let the sparsity promoting objective function f_2 be defined as,

$$f_2 = \sum_{n=1}^{N} \frac{\rho_k(n)}{\eta_k(n)}\widetilde{\mathbf{A}}_k(n,n), \tag{16}$$

where $\rho_k(n)$ corresponds to total energy consumed by n^{th} SN in transmission and sensing operations and $\eta_k(n)$ corresponds to its remaining energy during the k^{th} measurement cycle. The energy consumption by each SN is assumed to be known at the central entity. Motivation behind this assumption is that the sensing energy can be estimated from strength of the historical signals corresponding to the slowly varying pollution process, while the transmission energy can be calculated based on the distance between SN and mobile robot. Minimization of the second objective function f_2 considers current network resources and aims to reduce the number of active SNs, thereby reducing overall energy consumption of network and prolonging its life. Penalty associated with each SN promotes efficient utilization of network residual energy

by less penalizing the selection of SN with high remaining energy and low energy consumption requirement vis-à-vis the SN with low remaining energy and high energy consumption. Thus, jointly employing the BCRB and f_2, multi-objective optimization problem (MOP) for sensor selection during k^{th} measurement cycle is given by,

$$\begin{aligned}
\underset{\widetilde{\mathbf{A}}_k(n,n)\ \forall n}{\text{minimize}}\ & [\text{BCRB}, f_2] \\
\text{subject to}\ & \widetilde{\mathbf{A}}_k(n,n) \in \{0,1\},\ n=1,\ldots,N, && \text{(17a)} \\
& \widetilde{\mathbf{A}}_k(n,n) = 0,\ n \in \{i \mid \eta_k(i)=0\}, && \text{(17b)} \\
& \sum_{j\in\mathcal{R}_r} \widetilde{\mathbf{A}}_k(j,j) \geq 1,\ r=1,\ldots,R. && \text{(17c)}
\end{aligned}$$

Constraint (17a) has a straightforward implication of employing binary sensing matrix such that $\widetilde{\mathbf{A}}_k(n,n) = 1/0$ signifies active/sleep state of n^{th} SN. Constraint (17b) models a practical scenario wherein n^{th} SN will not participate in sensing during k^{th} cycle if its remaining energy $\eta_k(n) = 0$. Constraint (17c), referred to as coverage constraint, provides two-fold advantages. Firstly, it ensures activation of at least one SN from each coverage region $\mathcal{R}_r, \forall\ 1 \leq r \leq R$, assuming that location-aware densely deployed static WSN field is initially divided into total R fixed non-overlapping regions such that $\bigcup_{r=1}^{R} \mathcal{R}_r = \{1,\ldots,N\}$ with each region containing spatially proximal SNs. For instance, this can aid better monitoring of source(s) corresponding to the pollution process. Secondly, it provides a good blend of different features which represent the observed process more competently and thus help to improve the accuracy of estimation of signal across the entire field. The constraint (17c) along with the objective function f_2 prevents imbalance among selection of SNs, thereby eliminating coverage holes creation and reduced sensor lifetime problems. Note that, unlike the works [8], [17], [18], the MOP (17) does not assume fixed number of active SNs a priori. The active set $\mathcal{A}_k$ can be obtained from solution of the minimization problem (17) as,

$$\mathcal{A}_k = \left\{ n \mid \widetilde{\mathbf{A}}_k(n,n) = 1,\ \forall\ 1 \leq n \leq N \right\}. \qquad (18)$$

Due to the binary constraint (17a), the optimization problem (17) is non-convex in nature. Further, employing an exhaustive search over $\binom{N}{m}, \forall\ 1 \leq m \leq N$ combinations to optimize (17) is evidently impracticable for densely deployed WSNs. To reduce this computational complexity, the constraint (17a) is relaxed to well known convex box constraint, i.e., $\widetilde{\mathbf{A}}_k(n,n) \in [0,1], \forall n$, as demonstrated in [14], [39]. This converts the ensuing function f_2 from a non-convex weighted-l_0 norm function to a convex weighted-l_1 norm function. To solve the MOP (17), standard scalarization technique [40] is employed wherein scalar weight in the k^{th} cycle, $\lambda_k \in [0,1]$, is chosen based on predicted value of M_k such that, considering current network resources, the required reconstruction accuracy is always achieved as described later. The relaxed and scalarized optimization problem for sensor selection is now given by,

$$\begin{aligned}
\underset{\widetilde{\mathbf{A}}_k(n,n)\ \forall n}{\text{minimize}}\ & (1-\lambda_k)\,\text{Tr}\left\{ \left(\frac{1}{\sigma^2}\mathbf{B}_k^T \widetilde{\mathbf{A}}_k \mathbf{B}_k + \mathbf{\Gamma}_k^{-1} \right)^{-1} \right\} + \\
& \lambda_k \left(\sum_{n=1}^{N} \frac{\rho_k(n)}{\eta_k(n)} \widetilde{\mathbf{A}}_k(n,n) \right) \\
\text{subject to}\ & \widetilde{\mathbf{A}}_k(n,n) \in [0,1],\ n=1,\ldots,N, && \text{(19a)} \\
& \widetilde{\mathbf{A}}_k(n,n) = 0,\ n \in \{i \mid \eta_k(i)=0\}, && \text{(19b)} \\
& \sum_{j\in\mathcal{R}_r} \widetilde{\mathbf{A}}_k(j,j) \geq 1,\ r=1,\ldots,R. && \text{(19c)}
\end{aligned}$$

Note that the above optimization problem (19) is a convex problem which can be readily solved using a standard solver, such as CVX [41]. Further, the number of active SNs M_k and the active set $\mathcal{A}_k$ can be obtained from solution of the problem (19) as,

$$\begin{aligned}
M_k &= \text{round}\left(\sum_{n=1}^{N} \widetilde{\mathbf{A}}_k(n,n) \right), && \text{(20)} \\
\mathcal{A}_k &= \text{Row indices of } M_k \text{ largest elements of the ordered} \\
&\quad \text{set: } \left\{ \widetilde{\mathbf{A}}_k(n,n) \,|\, \widetilde{\mathbf{A}}_k(n,n) \geq \widetilde{\mathbf{A}}_k(m,m)\ \forall n,m \right\}. && \text{(21)}
\end{aligned}$$

One can even resort to rounding scheme wherein $\widetilde{\mathbf{A}}_k(n,n), \forall n$ are first rounded to nearest integer followed by computation of M_k and derivation of $\mathcal{A}_k$ as in [13], [16].

B. Feedback Mechanism for Adaptation

Intuition says that the sampling rate of a monitoring event should be dynamically adapted online to the streaming input signal variations. Even the authors in [21] experimentally illustrated this intuition by showing that in order to achieve relatively same error for different frequency sinusoidal input signal, a higher sampling rate is required for a rapidly varying (high frequency) signal and a low sampling rate suffice for slowly varying (low frequency) signal. This innate argument is emphasized in other pertinent works such as [7], [20], [24] as well. Further, it can be seen that if the sampling rate is not adapted (i.e. fixed λ is used in a way in MOP (19)), then as the measurement cycle progresses the fixed λ would give relatively more weightage to the decreasing energy based function f_2, due to which the BCRB value obtained on solving (19) and the corresponding MSE will keep increasing. Thus, motivated by these observations, the current section proposes a feedback-based sampling rate adaptation mechanism which predicts and updates the number of active SNs for the $(k+1)^{th}$ measurement cycle, denoted by $M_{k+1|k}$, based on both the estimation of signal variation (using the current k^{th} PCA-SBL based signal estimate $\widehat{\mathbf{x}}_k$) and the knowledge of network energy resources $\boldsymbol{\eta}_{k+1}, \boldsymbol{\rho}_{k+1}$ such that the estimation error always remains within the tolerance range of application. Note that the feedback mechanism is based on the presupposition that the underlying environmental phenomenon (air pollution here, as an example) is slowly varying, i.e. spatio-temporally correlated.

Let α and β be respectively the lower and upper limits of BCRB set as per the application requirements. The proposed adaptive feedback mechanism is built on the premise

that during each $(k+1)^{th}$ measurement cycle, the active set $\mathcal{A}_{k+1}$, obtained by considering $M_{k+1|k}$ based λ_{k+1} in (19), will always results in the corresponding $\text{BCRB}_{k+1} \in [\alpha, \beta]$. Initially set $M_{k+1|k} \leftarrow M_k$. In the proposed work, a heuristic ($\widehat{\delta}_k$) introduced in [7] is used to get an idea of signal variability. It approximates signal variations and reconstruction error in [7]. However, it cannot approximate the reconstruction error in the current scenario as, unlike system model in [7], the system model (5) herein considers noise as well. Therefore, the proposed work considers BCRB along with $\widehat{\delta}_k$ to approximate both the signal variations and quality. Based on this, the number of active nodes for next measurement cycle is adapted. The heuristic $\widehat{\delta}_k$ is given by,

$$\widehat{\delta}_k = \frac{\left\| \begin{bmatrix} \mathbf{y}_k \\ \mathbf{y}_{k-1} \end{bmatrix} - \begin{bmatrix} \mathbf{\Theta}_k \widehat{\mathbf{x}}_{k-1} \\ \mathbf{\Theta}_{k-1} \widehat{\mathbf{x}}_k \end{bmatrix} \right\|}{\left\| \begin{bmatrix} \mathbf{y}_k \\ \mathbf{y}_{k-1} \end{bmatrix} \right\|}. \tag{22}$$

During the k^{th} measurement cycle, the heuristic $\widehat{\delta}_k$ is computed using measurement vectors, estimated signal vectors, and estimated overcomplete dictionary matrices of the current k^{th} and the past $(k-1)^{th}$ measurement cycles. It is then compared against a suitable threshold δ_{th} and the predicted value $M_{k+1|k}$ is set as $M_{k+1|k} = (M_k + 1)$ if $\widehat{\delta}_k > \delta_{th}$. Analogously, for $\widehat{\delta}_k \leq \delta_{th}$, $M_{k+1|k}$ is obtained by appropriately decreasing M_k as described later. Note that, in the former case $M_{k+1|k}$ is increased in unit steps because the main aim of the proposed approach is to select sensors such that the network residual energy is utilized as judiciously as possible and the estimation performance remains within tolerance range. The increment step is also motivated by the work in [21], which experimentally demonstrated that sometimes for a large increase in the sampling rate the achievable reduction in error is small. Next, to quantify decrease in M_k for the latter case, define a heuristic $\widehat{\epsilon}_k$ called intracycle-variation as,

$$\widehat{\epsilon}_k = \left\| \widehat{\mathbf{x}}_k - \widehat{\mathbf{x}}_{k|M_k-i} \right\|, \tag{23}$$

where $\widehat{\mathbf{x}}_k$ and $\widehat{\mathbf{x}}_{k|M_k-i}$ respectively denote PCA-SBL estimate of the sparse signal vector $\mathbf{x}_k$ obtained by employing the current active set $\mathcal{A}_k$ with $|\mathcal{A}_k| = M_k$ and pruned active set $\mathcal{A}_{k|M_k-i}$ such that $|\mathcal{A}_{k|M_k-i}| = (M_k - i)$. The pruned active set $\mathcal{A}_{k|M_k-i}$ is constructed by removing i SNs from the set $\mathcal{A}_k$ having lowest magnitude of the reconstructed signal $\widehat{z}_k(.)$ across them such that at least one SN from each coverage region $R_r, \forall r$ is still present in the set. For instance, consider $N = 80$ SNs divided into $R = 8$ coverage regions, $\mathcal{R}_r = \{(r-1)\,10 + i,\ 1 \leq i \leq 10\},\ \forall\ 1 \leq r \leq 8$, and active set $\mathcal{A}_k = \{1, 5, 12, 18, 24, 37, 43, 56, 62, 77, 80\}$ with $|\widehat{z}_k(1)| \geq |\widehat{z}_k(5)| \geq |\widehat{z}_k(12)| \geq |\widehat{z}_k(18)| \geq |\widehat{z}_k(24)| \geq |\widehat{z}_k(37)| \geq |\widehat{z}_k(43)| \geq |\widehat{z}_k(56)| \geq |\widehat{z}_k(62)| \geq |\widehat{z}_k(77)| \geq |\widehat{z}_k(80)|$. Then, for $i = 2$ the pruned active set is $\mathcal{A}_{k|M_k-i} = \{1, 5, 12, 24, 37, 43, 56, 62, 77\}$. Let $\text{BCRB}_{k|M_k-i}$ be the BCRB evaluated using $\mathbf{A}_{k|M_k-i}$ based on the set $\mathcal{A}_{k|M_k-i}$. Initially set $i = 1$ and compute the heuristic $\widehat{\epsilon}_k$ using (23) and the $\text{BCRB}_{k|M_k-i}$ using (14). Thereafter, compare $\widehat{\epsilon}_k$ against an appropriately chosen threshold ϵ_{th} and if the conditions $\widehat{\epsilon}_k \leq \epsilon_{th}$ and $\text{BCRB}_{k|M_k-i} \in [\alpha, \beta]$ are satisfied simultaneously, then set $M_{k+1|k} = (M_k - i)$. Iterate the same process by increasing i in unit steps until either BCRB condition is violated, i.e. $\text{BCRB}_{k|M_k-i} \notin [\alpha, \beta]$ or the algorithm is unable to select at least one SN from R coverage regions each, i.e. $M_k - i < R$. The idea is to assess the extent to which the current value of M_k can be decreased for the $(k+1)^{th}$ cycle so that the resulting estimate $\widehat{\mathbf{x}}_{k|M_k-i}$ is not much different from the prior available benchmark $\widehat{\mathbf{x}}_k$ and the corresponding $\text{BCRB}_{k|M_k-i}$ still lies in the window $[\alpha, \beta]$. Further, this heuristic gives a rough idea of the spatial correlation of the process as it is observed in simulations that $\widehat{\epsilon}_k$ evaluates to even smaller values for scenarios with a higher spatial correlation (discussed in Section V-C). Thus, it can facilitate in tuning the adaptive framework according to different scenarios as well. At this juncture, one can see that consideration of the BCRB window is more generic as it can serve applications with strict single upper BCRB limit as well. However, considering too high/low single limit for BCRB might cause under/over sampling, whereas considering the BCRB window helps in adjusting the sampling rate appropriately even if the initial cycles have over/under sampled measurements.

Algorithm 1 Modified Binary Search

Input: $\boldsymbol{\rho}_{k+1}, \boldsymbol{\eta}_{k+1}, \mathbf{B}_{k+1}, M_{k+1|k}$.
Initialization: $[\lambda_L, \lambda_U] \leftarrow [0, 1]$.
while $\lambda_U - \lambda_L \geq \Delta$ **do**
  $\lambda_{k+1} = \frac{\lambda_L + \lambda_U}{2}$.
  Obtain $\widetilde{\mathbf{A}}_{k+1}$ by solving (19) using $\lambda_{k+1}, \boldsymbol{\rho}_{k+1}$, $\boldsymbol{\eta}_{k+1}, \mathbf{B}_{k+1}$.
  if $\sum_{n=1}^{N} \widetilde{\mathbf{A}}_{k+1}(n,n) > M_{k+1|k}$ **then**
    $\lambda_L \leftarrow \lambda_{k+1}$.
  else if $\sum_{n=1}^{N} \widetilde{\mathbf{A}}_{k+1}(n,n) < M_{k+1|k}$ **then**
    $\lambda_U \leftarrow \lambda_{k+1}$.
  else
    $break$.
  end if
end while
Output: $\widetilde{\mathbf{A}}_{k+1}, \lambda_{k+1}$.

So far, the number of SNs to be activated in the next measurement cycle is predicted considering solely the currently available and estimated signal vectors. Next, this predicted number $M_{k+1|k}$ is further updated considering the network energy resources during the $(k+1)^{th}$ measurement cycle. For this, the training set is updated as $\mathcal{T} = \mathcal{T} \bigcup \{\widehat{\mathbf{z}}_k\}$ using which the matrix $\mathbf{B}_{k+1}$ is updated as outlined in Section III-A. Thereafter, considering updated energy resource vectors $\boldsymbol{\eta}_{k+1}, \boldsymbol{\rho}_{k+1}$, and the updated matrix $\mathbf{B}_{k+1}$, the unknown scalar λ_{k+1} is found using modified binary search in $[\lambda_L, \lambda_U] = [0, 1]$ to minimize the optimization problem (19) with λ_{k+1} as an additional optimizing variable and $\lambda_U - \lambda_L < \Delta$ or $\sum_{n=1}^{N} \widetilde{\mathbf{A}}_{k+1}(n,n) = M_{k+1|k}$ as the stopping condition, where Δ is a small positive real number. Step-wise description of the modified binary search is presented in Algorithm 1. The active set $\mathcal{A}_{k+1}$, obtained by solving (19) using $M_{k+1|k}$ based λ_{k+1}, is further used for data acquisition if the corresponding

Algorithm 2 SBL-based adaptive sensing framework for WSN

Input: $\mathcal{T} = \{\mathbf{z}_{-K_{tr}+1}, \ldots, \mathbf{z}_{-1}, \mathbf{z}_0\}, \mathcal{R}_r \forall r, \alpha, \beta, \delta_{th}, \epsilon_{th}$.
Initialization: $\boldsymbol{\rho}_1, \boldsymbol{\eta}_1, \lambda_1, k = 1, exitflag = 0$.
while $exitflag == 0$ **do**
  if $k = 1$ **then**
    -Calculate $\bar{\mathbf{z}}_{\mathcal{T}}, \widehat{\boldsymbol{\Sigma}}_{\mathcal{T}}$ using (3), (4), estimate $\mathbf{B}_{k-1}$ using PCA scheme (Sec III-A); set $\mathbf{B}_k \approx \mathbf{B}_{k-1}$.
    -Solve (19) and construct $M_k, \mathcal{A}_k$ using (20), (21). Obtain $\mathbf{A}_k$ using (1).
  end if
  Broadcast sensing schedule $\mathcal{A}_k$ and collect $\mathbf{y}_k, \boldsymbol{\eta_{k+1}}$ from active SNs.
  Set $\boldsymbol{\Theta}_k = \mathbf{A}_k \mathbf{B}_k$.
  Compute $\widehat{\mathbf{x}}_k$ using SBL scheme given in Section III-B.
  Set $\widehat{\mathbf{z}}_k = \bar{\mathbf{z}}_{\mathcal{T}} + \mathbf{B}_k^T \widehat{\mathbf{x}}_k$.
  if $\sum_{n=1}^{N} \eta_{k+1}(n) > 0$ **then** `(Prediction starts)`
    Initialize $M_{k+1|k} \leftarrow M_k$.
    Compute $\widehat{\delta}_k$ using (22).
    if $\widehat{\delta}_k > \delta_{th}$ **then**
      $M_{k+1|k} \leftarrow M_k + 1$.
    else
      for $i = 1, \ldots, M_k - R$ **do**
        Construct $\mathcal{A}_{k|M_k-i}$, $\mathbf{A}_{k|M_k-i}$ using (1).
        Set $\boldsymbol{\Theta}_{k|M_k-i} = \mathbf{A}_{k|M_k-i} \mathbf{B}_k$.
        Obtain $\widehat{\mathbf{x}}_{k|M_k-i}$using SBL (Section III-B).
        Compute $\text{BCRB}_{k|M_k-i}$ using (14).
        Compute $\widehat{\epsilon}_k$ using (23).
        if $\widehat{\epsilon}_k \leq \epsilon_{th}$ and $\text{BCRB}_{k|M_k-i} \in [\alpha, \beta]$ **then**
          $M_{k+1|k} \leftarrow M_k - i$.
        else if $\text{BCRB}_{k|M_k-i} \notin [\alpha, \beta]$ **then** $break$.
        end if
      end for
    end if
    Update: $\mathcal{T} = \mathcal{T} \bigcup \{\widehat{\mathbf{z}}_k\}$. `(Update starts)`
    Compute $\bar{\mathbf{z}}_{\mathcal{T}}, \widehat{\boldsymbol{\Sigma}}_{\mathcal{T}}, \mathbf{B}_{k+1}$ as given in sec. III-A.
    do
      Call Algorithm 1- Modified Binary Search.
      if $\sum_{n=1}^{N} \widetilde{\mathbf{A}}_{k+1}(n,n) == M_{k+1|k}$ **then**
        Obtain $\mathcal{A}_{k+1}, \mathbf{A}_{k+1}$ using (21), (1).
        Calc. BCRB_{k+1} using $\mathbf{A}_{k+1}, \mathbf{B}_{k+1}$ in (14).
        if $\text{BCRB}_{k+1} < \alpha$ **then**
          $M_{k+1|k} \leftarrow \max\{M_{k+1|k} - 1, R\}$.
        else if $\text{BCRB}_{k+1} > \beta$ **then**
          $M_{k+1|k} \leftarrow \min\{M_{k+1|k} + 1, N\}$.
        end if
      else
        $exitflag \leftarrow 1$.
        $break$.
      end if
    while $\text{BCRB}_{k+1} \notin [\alpha, \beta]$.
    Update: $M_{k+1} \leftarrow M_{k+1|k}$.
  else
    $exitflag \leftarrow 1$.
  end if
  Update: $k \leftarrow k + 1$.
end while
Output: $K = k$.

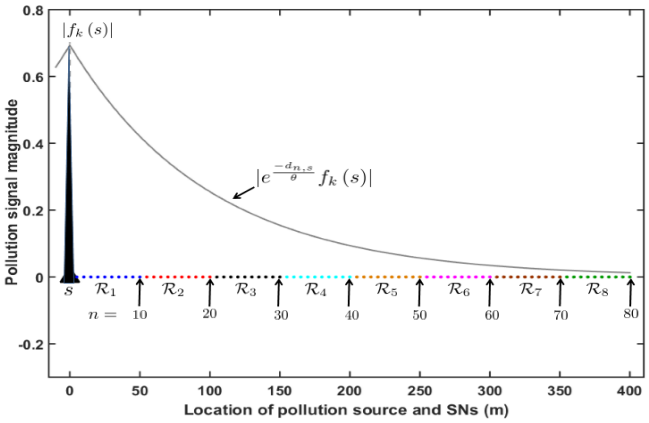

Fig. 1: Pictorial representation of spread of pollution signal in 1-dimensional space.

BCRB, denoted as BCRB_{k+1}, belongs to $[\alpha, \beta]$. Otherwise for the cases $\text{BCRB}_{k+1} < \alpha$ and $\text{BCRB}_{k+1} > \beta$, the value of $M_{k+1|k}$ is decreased and increased by one unit respectively and the process of searching λ_{k+1} and $\mathcal{A}_{k+1}$ is iterated until the achieved BCRB_{k+1} satisfies the condition, $\alpha \leq \text{BCRB}_{k+1} \leq \beta$. Further, the adaptation/measurement process stops during $(k+1)^{th}$ cycle either when the network energy is exhausted, i.e. $\sum_{n=1}^{N} \eta_{k+1}(n) = 0$ or when $\sum_{n=1}^{N} \widetilde{\mathbf{A}}_{k+1}(n,n) \neq M_{k+1|k}$ i.e. $\lambda_U - \lambda_L < \Delta$ which also models the scenario when even all the remaining alive SNs $(\eta_k(n) > 0)$ cannot fulfill the BCRB requirement. Note that from the beginning of monitoring process, it is ensured that $\text{BCRB}_{k+1}, \forall k$ corresponding to the active set $\mathcal{A}_{k+1}$ lies within the desired window $[\alpha, \beta]$ irrespective of the amount of increase or decrease in M_k to predict $M_{k+1|k}$. It is worth noting here that even in the absence of availability of the true MSE (13), the predicted feedback parameter $M_{k+1|k}$ and its updated version ensure that the network sensing quality does not go haywire at any point of time. Thus, the proposed adaptive framework for sensor selection has immense practical applicability.

A concise description of the SBL-based adaptive sensor selection framework is given in Algorithm 2 which outputs the total number of measurement cycles K that can be carried out by the proposed framework.

Complexity of the proposed adaptive framework is investigated in Section V-B, where the relative complexity of the competitive arts are also discussed.

V. Results and Discussion

This section illustrates the efficacy, tunability, and widespread practicability of the proposed adaptive sensing framework over the existing competitive ones in [7], [17], [18].

Consider a 1-dimensional WSN with $N = 80$ sensors equipped with non-rechargable batteries, equi-space deployed over a 400 m long field. $S = 1$ pollution source is located at the origin of the field, as shown in Fig. 1. The WSN field is divided into $R = 8$ continuous coverage regions each having 10 sensors, i.e. $\mathcal{R}_r = \{(r-1)10 + i, 1 \leq i \leq 10\}, \ \forall \ 1 \leq$

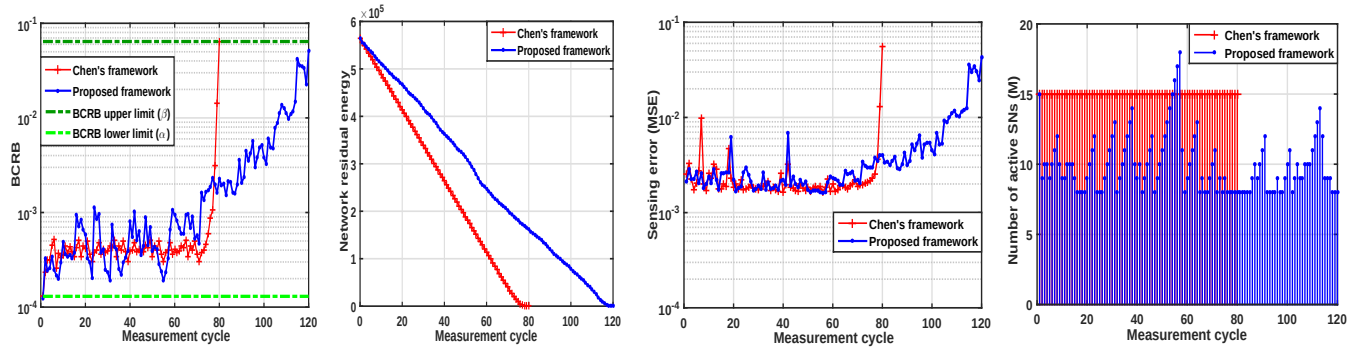

Fig. 2: Comparison of (a) BCRB, (b) network residual energy, (c) sensing error, and (d) number of active SNs of the proposed adaptive sensing framework with Chen's framework ($M_k = 15,\ \forall k$ measurement cycles) [17], [18]. Parameters are: $[\alpha, \beta] = \left[0.13 \times 10^{-3}, 64.19 \times 10^{-3}\right], \delta_{th} = 0.11, \epsilon_{th} = 2.5 \times 10^{-5}$, and $\lambda_1 = 0.52$ in (19).

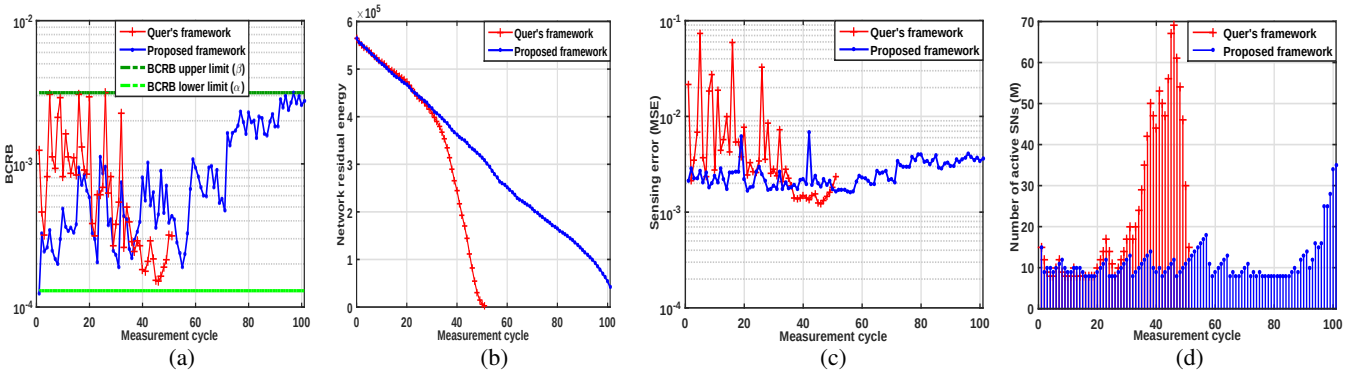

Fig. 3: Comparison of (a) BCRB, (b) network residual energy, (c) sensing error, and (d) number of active SNs of the proposed adaptive sensing framework with Quer's framework ($C_1 = 1.2, C_2 = 3, p_{tx} = 0.1$) [7]. The parameters are: $[\alpha, \beta] = \left[0.13 \times 10^{-3}, 3.14 \times 10^{-3}\right], \delta_{th} = 0.11, \epsilon_{th} = 2.5 \times 10^{-5}$, and $M_1 = 15$.

$r \leq R$. Note that, this equidistant deployment based 1-dimensional simulation setting is considered just for simplicity and better understanding of analysis. However this could be easily extended to 2-dimensional setting with non-uniform node deployment for monitoring multiple pollution sources located anywhere in the field. For $k = 1$, the pollution signal $f_1(s)$ emitted from each monitored source $s, 1 \leq s \leq S$, is generated as an independent univariate real Gaussian [29], [42] with zero mean and variance $\sigma_f^2(s) = 1$ except for simulation Section V-E. For $k > 1$, the temporal samples of $f_k(s)$ are generated using AR(1) process [43] as $f_k(s) = \phi f_{k-1}(s) + \sqrt{1-\phi^2} w_k(s)$, where $w_k(s) \sim \mathcal{N}\left(0, \sigma_f^2(s)\right)$ and ϕ denotes temporal correlation coefficient between two consecutive samples. The pollution signal sensed by the n^{th} SN in k^{th} cycle is obtained as $z_k(n) = \sum_{s=1}^{S} e^{\frac{-d_{n,s}}{\theta}} f_k(s)$ [44] where $d_{n,s}$ and θ denote the distance between n^{th} sensor and s^{th} source and the spatial diffusion/correlation parameter of the source, respectively. Similarly as in [16], the noise variance is fixed as $\sigma^2 = 10^{-5}$. This choice is required to guarantee a reasonable sensing performance in the underlying severely ill-posed estimation scenarios $(N/M_k \gg 2)$ presented in the subsections below. Except for the simulation settings in Section V-C, dynamics of the pollution process are considered as $\theta = 100$ and $\phi = 0.99$. During each k^{th} cycle, the sparsifying matrix $\mathbf{B}_k$ is estimated using $\mathcal{T} = \{\mathbf{z}_{-4}, \mathbf{z}_{-3}, \ldots, \mathbf{z}_0, \widehat{\mathbf{z}}_1, \ldots, \widehat{\mathbf{z}}_{k-1}\}$ where $K_{tr} = 5$ cycles are used for initial training. Note that, the works such as [8], [17], [18] generate the sparse signal $\mathbf{x}_k$ based on assumed sparsity and Gaussian matrix $\mathbf{B}_k$ separately. However, the synthetic data used herein embody the effect of the pollution process dynamics to generate the signal sensed by SNs $\mathbf{z}_k$ from which the matrix $\mathbf{B}_k$ is estimated. Subsequently a sparse representation is given as $\mathbf{z}_k = \mathbf{B}_k \mathbf{x}_k$ without any a priori assumption of sparsity. Thus, the framework validated on this synthetic data can be readily applied to any real data obtained from WSN monitoring slowly varying process. The matrix $\mathbf{\Gamma}_k$ in (19) is set as a diagonal matrix having eigen values of the matrix $\widehat{\mathbf{\Sigma}}_{\mathcal{T}}$ as its diagonal elements[1]. The initial energy of each SN is set as $\eta_1(n) \in [7000, 7100]$ units, $\forall n$ and the combined sensing and transmission energy is fixed as $\rho_k(n) = 500$ units, $\forall n, \forall k$. After each measurement cycle k, the residual energy for next $(k+1)^{th}$ cycle is updated as $\eta_{k+1}(n) = \eta_k(n) - \rho_k(n),\ \forall n, \forall k$. The initial hyperparameter estimates and the convergence accuracy of the SBL scheme are set respectively as, $\gamma_k^{(0)}(n) = 1, \forall n, \forall k$ [30] and $\left\| \boldsymbol{\gamma}_k^{(l+1)} - \boldsymbol{\gamma}_k^{(l)} \right\| \leq 10^{-7}$. Performance metrics used in the

[1] $E\{\mathbf{x}_k \mathbf{x}_k^T\} = E\{\mathbf{B}_k^T \mathbf{z}_k \mathbf{z}_k^T \mathbf{B}_k\} = \mathbf{B}_k^T E\{\mathbf{z}_k \mathbf{z}_k^T\} \mathbf{B}_k \approx \mathbf{B}_k^T \widehat{\mathbf{\Sigma}}_{\mathcal{T}} \mathbf{B}_k = \mathbf{B}_k^T \left(\mathbf{B}_k \mathbf{\Gamma}_k \mathbf{B}_k^T\right) \mathbf{B}_k = \mathbf{\Gamma}_k$.

simulation plots are, sensing error (MSE) $= \left\|\mathbf{x}_k - \widehat{\mathbf{x}}_k\right\|^2 = \left\|\mathbf{z}_k - \widehat{\mathbf{z}}_k\right\|^2$ and network residual energy $= \sum_{n=1}^{N} \eta_k(n)$. For each measurement cycle, the sensing performance is averaged over 300 montecarlo iterations. Objective functions of the scalarized multi-objective sensing problem (19) are normalized using their smallest possible values as, $\frac{\mathrm{Tr}\left(\frac{1}{\sigma^2}\mathbf{B}_k^T\widetilde{\mathbf{A}}_k\mathbf{B}_k+\mathbf{\Gamma}_k^{-1}\right)^{-1}}{\mathrm{Tr}\left(\frac{1}{\sigma^2}\mathbf{B}_k^T\mathbf{I}_N\mathbf{B}_k+\mathbf{\Gamma}_k^{-1}\right)^{-1}}$ and $\frac{\left(\sum_{n=1}^{N}\frac{\rho_k(n)}{\eta_k(n)}\widetilde{\mathbf{A}}_k(n,n)\right)}{\left(\sum_{n\in\mathcal{E}}\frac{\rho_k(n)}{\eta_k(n)}\widetilde{\mathbf{A}}_k(n,n)\right)}$, where $\mathcal{E}$ is the set containing indices corresponding to R highest remaining energy SNs, one from each coverage region $\mathcal{R}_r$. CVX optimization tool [41] is used for solving the scalarized and relaxed convex sensing problem (19). The parameter Δ in the stopping criteria of modified binary search is set as $\Delta = 10^{-4}$.

A. Performance Comparison with Different Non-adaptive and Adaptive Sensing Techniques

Figs. 2(a)-(c) compare performance of the proposed sensing framework with that of the closest non-adaptive framework developed by Chen *et al.* in [17], [18]. It can be observed from the Figs. 2(a)-(c) that the proposed framework provides significant improvement in energy efficiency without compromising on the sensing accuracy by increasing network's lifetime by ≈ 40 measurement cycles over the other for the same range of BCRB $\in \left[0.13\times10^{-3}, 64.19\times10^{-3}\right]$. This gain, as shown in Fig. 2(d), is due to the adaptation of sampling rate.

Similarly, Figs. 3(a)-(c) illustrate that the proposed adaptive sensing framework achieves superior energy efficiency and stable sensing quality over the closest adaptive framework developed by Quer *et al.* [7]. As captured in Fig. 3(d), the improvement in network lifetime (≈ 50 cycles) of the proposed scheme is attributed to more accurate quantification of increase or decrease in the sampling rate, while stable sensing performance is due to optimized active set selection.

The sensing performance achieved in Figs. 2(c) and 3(c) is within the acceptable working range as suggested in works [17], [45], which further corroborates the appropriateness of BCRB as one of the performance measures in problem (19). Note that, in relative performance evaluations, the proposed framework's parameters $[\alpha, \beta]$ are set as per the minimum and maximum BCRB achieved in the respective competitive schemes; $\delta_{th}, \epsilon_{th}$ are set such that the variations of the pollution signal are captured effectively; and λ_1 in (19) is set such that the active number of sensors during $k = 1$ measurement cycle, i.e. M_1, is same for all the schemes. Further, for fair comparison of energy efficiency performance, SBL-based recovery scheme is employed in both Chen's and Quer's sensing frameworks as well, and correspondingly BCRB is used as performance measure in Chen's scheme.

Further, note that, slight increase in error in last measurement cycles in Figs. 2(c) and 3(c) is due to the components of active set selected in the last cycles. After execution of many measurement cycles, remaining energy of the SNs near pollution source (cf. Fig. 1) is exhausted as they are activated more frequently compared to far-off nodes. As a result, the nodes away from the pollution source are progressively selected for the sample measurement. The measurements of far-off nodes selected in last few cycles do not recover the process across all SNs as competently as done by the near-by SNs. Due to this the sensing error increases slightly in the last few cycles. In fact, in simulations with strict upper limit of BCRB (i.e., lesser value of β), the slight increase in MSE in last measurement cycles is not even seen, as observed from Figs. 4(c) and 5(c).

Remark 1. *These performance results demonstrate that, the proposed adaptive and optimized sparse sensor selection for monitoring a slowly varying process helps in realizing energy-efficient sensing for IoT applications.*

B. Complexity Analysis

The main focus of the work is to propose an energy-efficient adaptive sensing framework based on an efficient recovery scheme. Therefore, let the generalized complexity of recovery scheme be denoted by $\mathcal{O}_{Rec}$. The complexity of the proposed framework is obtained by calculating complexities of the prediction and the update steps in one measurement cycle. The prediction step involves computation of $\widehat{\delta}_k$ and $M_{k+1|k}$ which have complexities $\mathcal{O}(M_k N)$ and $\mathcal{O}\left((M_k-1)^3\right)$, respectively. Note that the latter part considers the worst case wherein the for loop corresponding to $\widehat{\delta}_k \leq \delta_{th}$ runs $(M_k - R)$ times. Thus, the overall complexity of the prediction step evaluates to $\approx \left(\mathcal{O}\left((M_k-1)^3\right) + \mathcal{O}_{Rec}\right)$. In the update step, calculation of $\bar{\mathbf{z}}_{\mathcal{T}}, \widehat{\mathbf{\Sigma}}_{\mathcal{T}}$, and $\mathbf{B}_{k+1}$ has combined complexity $\mathcal{O}\left(N^2\right)$. The modified binary search converges in $\log_2\left(\frac{\lambda_U^{(1)}-\lambda_L^{(1)}}{\Delta}\right)$ iterations with each solving sensor selection problem (19) using CVX tool. CVX employs infeasible primal-dual predictor-corrector interior point algorithm based on HKM search direction having complexity $\approx \mathcal{O}\left(\widetilde{N}\log\left(\frac{1}{\nu}\right)\right)$ [46], where $\widetilde{N}$ denotes the number of variables after converting problem (19) to standard form by CVX and ν denotes the precision accuracy (10^{-8} by default). Further, the update steps of $M_{k+1|k}$ has $\mathcal{O}\left((M_{k+1|k})^3\right)$ complexity. In the worst case, the update step will converge in $\left(M_{k+1|k} - R + 1\right)$ iterations, and thus its complexity is $\approx \left(\mathcal{O}\left((M_{k+1|k})^3\right) + \left(M_{k+1|k} - R + 1\right)\log_2\left(\frac{1}{\Delta}\right)\mathcal{O}\left(\widetilde{N}\log\left(\frac{1}{\nu}\right)\right)\right)$. Hence, the combined complexity of the proposed adaptive sensing framework is $\approx \Big(\mathcal{O}_{Rec} + \mathcal{O}\left((M_{k+1|k})^3\right) + \left(M_{k+1|k} - R + 1\right)\log_2\left(\frac{1}{\Delta}\right)\mathcal{O}\left(\widetilde{N}\log\left(\frac{1}{\nu}\right)\right)\Big)$. Note that the number of iterations required for convergence of the prediction and the update steps depend on the BCRB window $[\alpha, \beta]$ required by application, especially during last few measurement cycles when network energy is about to exhaust. As observed in two simulation settings considered in Section V-A, for a wide window these steps converge fast compared to the case with a narrow window. Also, the above complexities are computed by considering a less complex expression for equation (14) which is obtained by employing matrix inversion lemma [36] as BCRB $= \mathrm{Tr}\left\{\mathbf{\Gamma}_k - \mathbf{\Gamma}_k\mathbf{B}_k^T\mathbf{A}_k^T\left(\sigma^2\mathbf{I}_{M_k} + \mathbf{A}_k\mathbf{B}_k\mathbf{\Gamma}_k\mathbf{B}_k^T\mathbf{A}_k^T\right)^{-1}\mathbf{A}_k\mathbf{B}_k\mathbf{\Gamma}_k\right\}$.

On the similar lines, the complexity of the closest non-adaptive and optimized selection based Chen's schemes [17], [18] evaluate to $\approx \left(\mathcal{O}_{Rec} + \mathcal{O}\left(\widetilde{N}\log\left(\frac{1}{\nu}\right)\right)\right)$ and that of the

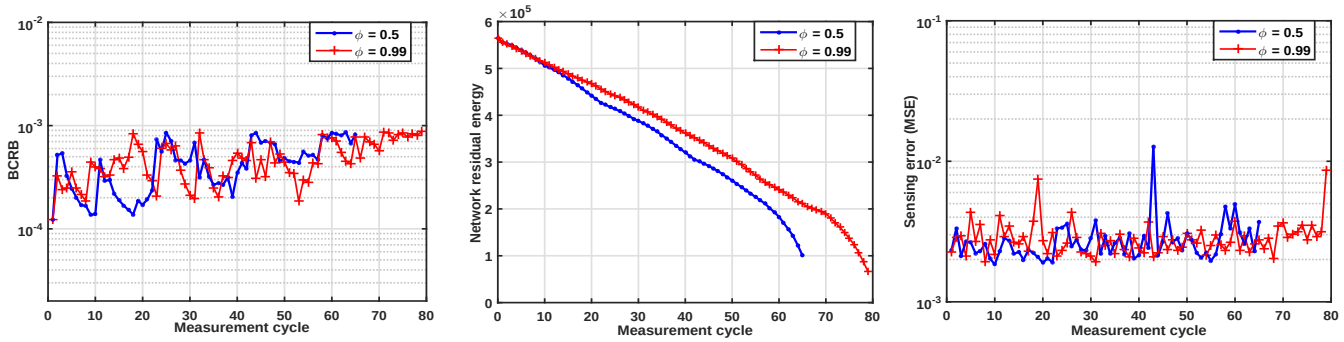

(a) (b) (c)

Fig. 4: Performance of the proposed adaptive sensing framework in terms of (a) BCRB, (b) network residual energy, and (c) sensing error at different temporal dynamics: $\phi = 0.5$ and $\phi = 0.99$ of the pollution process. The common parameters are: $[\alpha, \beta] = \left[0.13 \times 10^{-3}, 0.876 \times 10^{-3}\right], \delta_{th} = 0.11, \epsilon_{th} = 4 \times 10^{-5}, \lambda_1 = 0.52$, and $\theta = 100$.

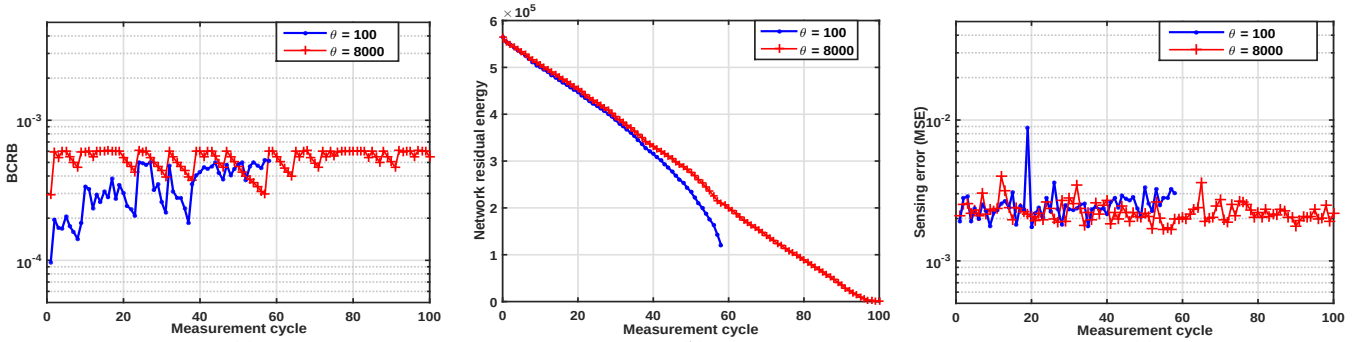

(a) (b) (c)

Fig. 5: Performance of the proposed adaptive sensing framework in terms of (a) BCRB, (b) network residual energy, and (c) sensing error at different spatial diffusion parameter of the pollution process: $\theta = 100$ and $\theta = 8000$ with $[\alpha, \beta] = \left[0.097 \times 10^{-3}, 0.52 \times 10^{-3}\right]$ and $\left[0.2928 \times 10^{-3}, 0.62 \times 10^{-3}\right]$, respectively. The common parameters $\delta_{th} = 0.11, \epsilon_{th} = 1.25 \times 10^{-5}, \lambda_1 = 0.6$, and $\phi = 0.99$.

TABLE I: Comparison of network lifetime and complexity.

$[\alpha, \beta] \times 10^{-3}$	Framework	Network lifetime (K cycles)	T_{comp} (min)	$\mathrm{T}_{overall}$ (min)
$[0.13, 64.19]$ (wide window)	Proposed	120	1.61	1.77
	Chen's	80	0.63	0.63
$[0.13, 3.14]$ (narrow window)	Proposed	101	1.76	1.94
	Quer's	51	0.58	0.58

closest adaptive and random selection based Quer's scheme [7] evaluates to $\approx (\mathcal{O}_{Rec} + \mathcal{O}(M_k N))$.

In Table I, average time per cycle- comparison and overall, denoted by T_{comp} and $\mathrm{T}_{overall}$, are calculated as $\frac{1}{K_{case}} \sum_{k=1}^{K_{case}} t_k$, where t_k, K_{case} represent time required in execution of k^{th} measurement cycle and total number of considered cycles, respectively. For $\mathrm{T}_{overall}$, $K_{case} = K$, while for T_{comp} it is set as per total cycles of the scheme with minimum lifetime, i.e. $K_{case} = 80$ and $K_{case} = 51$, respectively, for comparison of the proposed scheme with Chen's and Quer's schemes. The value of the parameters mentioned in the Table I are obtained by simulating the WSN model described in Sections V and V-A in Matlab R2015a on Intel i7-6700 CPU with 3.4 GHz clock and 32 GB RAM.

The complexity expressions and the results in Table I indicate that the intelligence imparted by the proposed SBL-based adaptive sensing framework gives respectively 1.5 and 2 folds increase in energy efficiency/lifetime over Chen's and Quer's schemes at the cost of an increased complexity as seen from the values of parameter T_{comp}. However, the complexity can be handled by providing powerful computational hardware to the central entity during the WSN deployment. The energy efficiency is a critical aspect as network energy, provided to SNs during deployment through high capacity non-rechargeable batteries, once exhausted cannot be easily replenished in a large scale WSN deployment.

Remark 2. *Thus, the proposed framework trades-off complexity at the central entity to increase lifetime of SNs.*

C. Effect of Dynamics of the Monitored Pollution Process

Temporal dynamics: For this study, two scenarios are considered with temporal correlation coefficients of the pollution process given by $\phi = 0.5$ and $\phi = 0.99$. Figs. 4(a)-(c) indicate that the former case with higher temporal variations consumes network energy at a faster rate than that in the latter case with lower temporal variations, which is due to frequent required adaptation in sampling rate while maintaining a predefined sensing quality.

Spatial dynamics: This study compares two cases with the spatial diffusion parameters set as $\theta = 100$ and $\theta = 8000$.

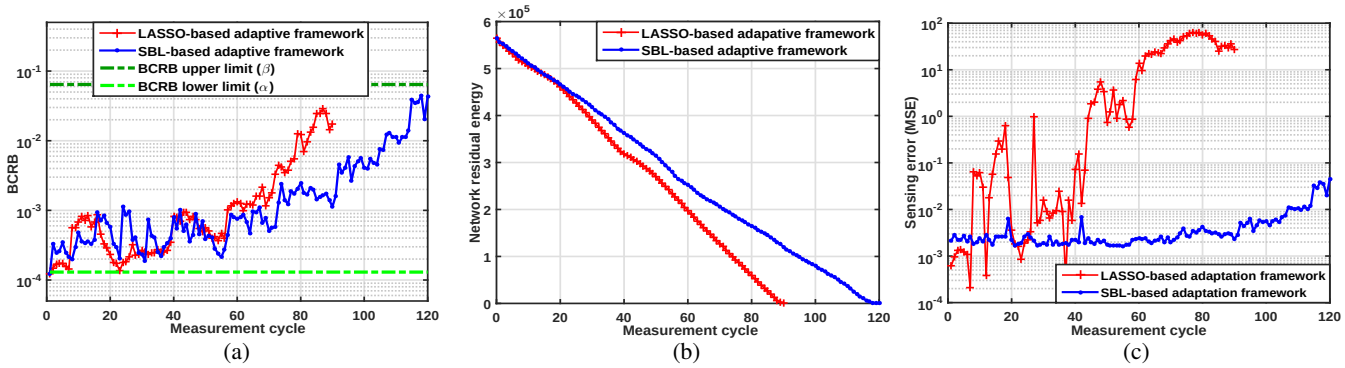

Fig. 6: Comparison of the performance measures, namely, (a) BCRB, (b) network residual energy, and (c) sensing error, achieved by integrating the proposed adaptive sensing framework with different recovery schemes: LASSO [26] and SBL [29]. The system parameters are: $[\alpha, \beta] = \left[0.13 \times 10^{-3}, 64.19 \times 10^{-3}\right], \delta_{th} = 0.11, \epsilon_{th} = 2.5 \times 10^{-5}$, and $\lambda_1 = 0.52$.

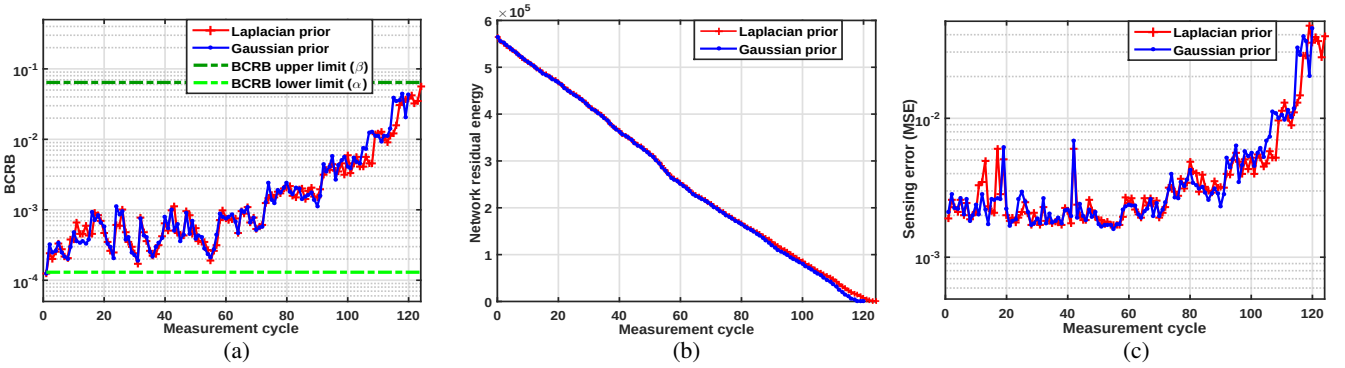

Fig. 7: Comparison of (a) BCRB, (b) network residual energy, and (c) sensing error measures of the proposed SBL-based adaptive sensing framework used for monitoring Laplacian and Gaussian pollution processes, with the parameters $[\alpha, \beta] = \left[0.13 \times 10^{-3}, 64.19 \times 10^{-3}\right], \delta_{th} = 0.11, \epsilon_{th} = 2.5 \times 10^{-5}$, and $\lambda_1 = 0.52$.

To compare energy efficiency while maintaining same sensing performance, the BCRB window ($[\alpha, \beta]$) for $\theta = 100$ is set as $\left[0.097 \times 10^{-3}, 0.52 \times 10^{-3}\right]$, while it is considered as $\left[0.2928 \times 10^{-3}, 0.62 \times 10^{-3}\right]$ for $\theta = 8000$ case. Figs. 5(a)-(c) illustrate that the network energy efficiency and hence the lifetime is more in the latter case with slow spatial variations as compared to the former case. This observation matches well with intuition that a low sampling rate suffices to provide the desired reconstruction performance in a slowly varying process. Further, this shows that the proposed sensing framework is tunable to different practical scenarios. It is experimentally observed that for $\theta = 8000$ case, $\widehat{\delta}_k$ evaluates to value $\approx 10^{-6}$ in most of the measurement cycles. Thus, the parameter δ_{th} is appropriately set as 1.25×10^{-5} for comparing the considered cases with different θ. Another interesting observation is that for $\theta = 8000$, the active set $\mathcal{A}_k$ obtained during each measurement cycle k has a comparatively good mixture of SNs from all the coverage regions $\mathcal{R}_r, \forall r$ due to which the BCRB is obtained within the set limits until the network energy resource is completely exhausted.

Remark 3. *With the proposed approach, the WSN can appropriately adapt sensing of a spatio-temporally varying process for increased network lifetime without compromising on the sensing quality.*

D. Sensitivity of the Proposed Framework to Different Recovery Schemes

This section employs LASSO (basis pursuit denoising) recovery scheme [26] with the proposed adaptive framework and investigates its performance. It can be observed from Figs. 6(a)-(c) that the LASSO-based adaptation provides poor sensing quality (MSE) and lower energy efficiency compared to the SBL-based adaptation. This observation emphasizes the need of a recovery algorithm that provides maximally sparse solution so that a reliable feedback can be provided in the framework and thus validates the choice of SBL scheme for the proposed framework.

Remark 4. *An efficient recovery algorithm plays a vital role in designing an energy-efficient adaptive sensing framework as exemplified by the SBL scheme used in the proposed adaptive framework.*

E. Applicability of SBL-based Adaptive Sensing Framework to Non-Gaussian Monitoring Process

Consider the pollution signal $f_k(s)$ drawn from an IID Laplacian distribution [35]. It is observed from Figs. 7(a)-(c) that employing parameterized Gaussian prior-based SBL technique for adaptively sensing a non-Gaussian pollution process gives the energy efficiency and the sensing performance similar to the case of sensing Gaussian process.

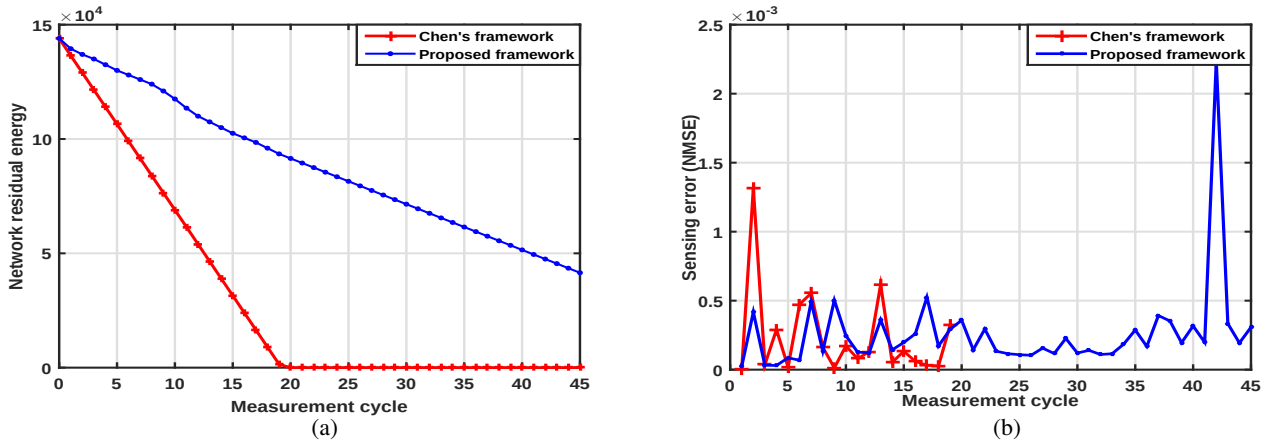

Fig. 8: Comparison of (a) network residual energy, and (b) sensing error of the proposed adaptive sensing framework with Chen's framework ($M_k = 15$, $\forall k$ measurement cycles) [17], [18]. Parameters are: $[\alpha, \beta] = \left[2.1383 \times 10^{-5}, 14.9 \times 10^{-3}\right]$, $\delta_{th} = 0.03, \epsilon_{th} = 0.5$, and $\eta_1(n) = 4500$ units $\forall n$.

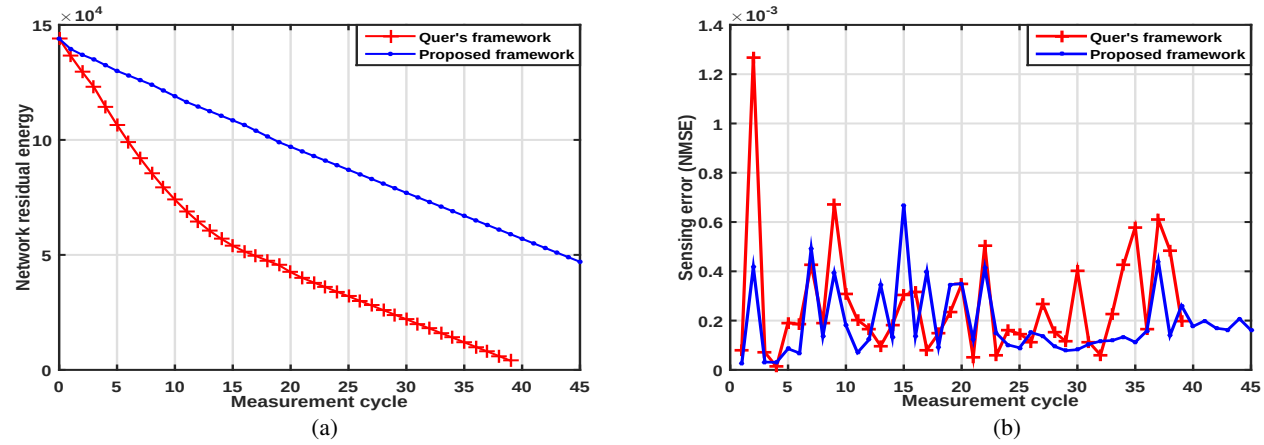

Fig. 9: Comparison of (a) network residual energy, and (b) sensing error of the proposed adaptive sensing framework with Quer's framework ($C_1 = 1.2903, C_2 = 1.2, p_{tx} = 0.125$) [7]. The parameters are: $[\alpha, \beta] = \left[2.1628 \times 10^{-5}, 0.0522\right]$, $\delta_{th} = 0.03, \epsilon_{th} = 0.5$, $M_1 = 15$, and $\eta_1(n) = 4500$ units $\forall n$.

Remark 5. *This result has widespread practical applicability, as it shows that the proposed SBL-based adaptive sensing framework does not necessarily fail altogether in continuously monitoring pollution process with different prior distributions.*

F. Performance study of the proposed approach using real WSN data set

For performance comparison using real signal, humidity data collected by a WSN located in Intel Berkeley research lab [47] is considered. Measurements of a subset of 32 nodes sensed over the same time duration are used. The lab area covered by the considered 32 nodes is divided into $R = 4$ regions. The noise variance is set as $\sigma^2 \approx 10^{-6}$. Other parameters such as $\eta_1(n)$, $\forall n$, δ_{th}, and ϵ_{th} are respectively set as 4500 units, 0.03, and 0.5. Performance metric used in the simulation plots are NMSE$= \frac{\|\mathbf{x}_k - \widehat{\mathbf{x}}_k\|^2}{\|\mathbf{x}_k\|^2}$ and network residual energy$= \sum_{n=1}^{N} \eta_k(n)$. The NMSE is used herein as it gauges the energy in error against the signal's energy. However, it is important to note that the metric NMSE has not been used in the framework directly as the WSN signal $\mathbf{x}_k$ is unknown. It is used just for comparative performance study of the proposed framework. It can be observed from Figs. 8 and 9 that the proposed adaptive sensor selection framework is more energy-efficient compared to the existing non-adaptive framework developed by Chen *et al.* [17], [18] and adaptive one developed by Quer *et al.* [7]. It can also be noted that, in the proposed framework sensing quality has not been compromised/sacrificed to improve network lifetime.

VI. Conclusion

This paper has proposed a novel SBL-based adaptive sensing framework for a densely deployed static WSN. The framework exploits spatial and temporal correlation of the underlying monitored phenomenon to dynamically adjust the instance of sampling event at the sensors for smart data acquisition in IoT applications. For sensor selection, a multi-objective optimization problem has been formulated which jointly maximizes two conflicting performance measures: sensing quality and energy efficiency of the network. For online

adaptation, a feedback mechanism has been embedded which predicts and updates the set of participating sensors for the next measurement cycle based on the estimation of signal variability and current energy parameters of the sensors such that the sensing error is within an acceptable limit. Further, this work has investigated efficacy of the joint PCA-SBL scheme in providing a good estimate of the inherently sparse signal of WSN which determines reliability of the feedback mechanism in the adaptation framework. Through simulation study that uses both real and synthetic data of a WSN, it has been illustrated that the proposed sensing framework provides superior energy efficiency which significantly increases the network lifespan while maintaining a stable sensing quality. Further, it has been demonstrated that the proposed scheme is easily tunable to different application requirements and dynamics of the monitored phenomenon. Future work may reduce complexity of the proposed adaptive sensing framework and explore its implementation in a decentralized manner.

APPENDIX A
BAYESIAN CRAMÉR-RAO BOUND (BCRB)

Using the signal model in (5), the BCRB, which characterizes the MSE in estimate of the unknown vector $\mathbf{x}_k \in \mathbb{R}^{N\times 1}$, is computed as $\text{BCRB} = \text{Tr}\left\{\mathbf{J}_B^{-1}\right\}$, with $\mathbf{J}_B \in \mathbb{R}^{N\times N}$ being the Bayesian Fisher information matrix (FIM) [36] given by,

$$\mathbf{J}_B = \underbrace{-\text{E}_{(\mathbf{y}_k,\mathbf{x}_k)}\left\{\frac{\partial^2 \mathcal{L}(\mathbf{y}_k|\mathbf{x}_k;\mathbf{\Gamma}_k)}{\partial \mathbf{x}_k \partial \mathbf{x}_k^T}\right\}}_{\mathbf{J}_D} \underbrace{-\text{E}_{(\mathbf{x}_k)}\left\{\frac{\partial^2 \mathcal{L}(\mathbf{x}_k;\mathbf{\Gamma}_k)}{\partial \mathbf{x}_k \partial \mathbf{x}_k^T}\right\}}_{\mathbf{J}_P}, \quad (24)$$

where the quantities $\mathcal{L}(\mathbf{y}_k|\mathbf{x}_k;\mathbf{\Gamma}_k), \mathcal{L}(\mathbf{x}_k;\mathbf{\Gamma}_k)$ and $\mathbf{J}_D, \mathbf{J}_P$ denote the log-likelihood functions of the vectors $\mathbf{y}_k$, $\mathbf{x}_k$ parameterized by $\mathbf{\Gamma}_k$ and $(N \times N)$ sized FIMs with respect to $\mathbf{y}_k, \mathbf{x}_k$ respectively. Using the prior distribution of the vector $\mathbf{x}_k$ from (6), the log-likelihood evaluates to $\mathcal{L}(\mathbf{x}_k) = \left(\widetilde{k} - \frac{1}{2}\mathbf{x}_k^T {\mathbf{\Gamma}_k}^{-1}\mathbf{x}_k\right)$, where $\widetilde{k}$ denotes a parametric constant. Further, considering the second order derivative of $\mathcal{L}(\mathbf{x}_k;\mathbf{\Gamma}_k)$ with respect to $\mathbf{x}_k$ yields $\frac{\partial^2 \mathcal{L}(\mathbf{x}_k)}{\partial \mathbf{x}_k \partial \mathbf{x}_k^T} = \mathbf{\Gamma}_k^{-1}$, and thus the FIM matrix $\mathbf{J}_P$ evaluates to $\mathbf{J}_P = \mathbf{\Gamma}_k^{-1}$. Next, the log-likelihood function $\mathcal{L}(\mathbf{y}_k;\mathbf{x}_k)$ for the measurement vector $\mathbf{y}_k$ after ignoring the constant terms is given as, $\mathcal{L}(\mathbf{y}_k|\mathbf{x}_k;\mathbf{\Gamma}_k) = \frac{1}{2\sigma^2}\|\mathbf{y}_k - \mathbf{A}_k\mathbf{B}_k\mathbf{x}_k\|^2$. Thus, the FIM $\mathbf{J}_D$ can be evaluated as, $\mathbf{J}_D = \frac{1}{\sigma^2}\mathbf{B}_k^T\mathbf{A}_k^T\mathbf{A}_k\mathbf{B}_k$ with the final BCRB expression given by,

$$\text{BCRB} = \text{Tr}\left\{\left(\frac{1}{\sigma^2}\mathbf{B}_k^T\mathbf{A}_k^T\mathbf{A}_k\mathbf{B}_k + {\mathbf{\Gamma}_k}^{-1}\right)^{-1}\right\}. \quad (25)$$

APPENDIX B
CONVEXITY OF BCRB OBJECTIVE FUNCTION

BCRB expression in (14) can be written as $f(\mathbf{J}_B) = \text{Tr}\left(\mathbf{J}_B^{-1}\right)$. Convexity of $f(\mathbf{J}_B)$ can be proved using proposition outlined in [39] which states that *the function f is convex iff for all $\mathbf{J}_B \in$ **dom** $f = \mathbb{S}_{++}^N$ and all $\mathbf{V} \in \mathbb{S}^N$, the function $g(t) = f(\mathbf{J}_B + t\mathbf{V})$ is convex in its domain $\{t|\mathbf{J}_B + t\mathbf{V} \in$ **dom** $f\}$*. Now,

$$\begin{aligned} g(t) &= \text{Tr}\left((\mathbf{J}_B + t\mathbf{V})^{-1}\right) \\ &= \text{Tr}\left(\mathbf{J}_B^{-1/2}\left(\mathbf{I}_N + t\mathbf{J}_B^{-1/2}\mathbf{V}\mathbf{J}_B^{-1/2}\right)^{-1}\mathbf{J}_B^{-1/2}\right) \\ &= \text{Tr}\left(\mathbf{J}_B^{-1}\mathbf{Q}\left(\mathbf{I}_N + t\mathbf{\Lambda}\right)^{-1}\mathbf{Q}^T\right) \\ &= \text{Tr}\left(\mathbf{Q}^T\mathbf{J}_B^{-1}\mathbf{Q}\left(\mathbf{I}_N + t\mathbf{\Lambda}\right)^{-1}\right) \\ &= \sum_{n=1}^{N}\left(\mathbf{Q}^T\mathbf{J}_B^{-1}\mathbf{Q}\right)_{n,n}(1 + t\lambda_n)^{-1}, \end{aligned} \quad (26)$$

where eigenvalue decomposition $\mathbf{J}_B^{-1/2}\mathbf{V}\mathbf{J}_B^{-1/2} = \mathbf{Q}\mathbf{\Lambda}\mathbf{Q}^T$ [36] and matrix trace property $\text{Tr}(\mathbf{CD}) = \text{Tr}(\mathbf{DC})$ [37] are used. The function $g(t)$ is convex since it is expressed as weighted sum of convex functions $(1 + t\lambda_n)^{-1}$ where the weights $\left(\mathbf{Q}^T\mathbf{J}_B^{-1}\mathbf{Q}\right)_{n,n}$ are positive.

REFERENCES

[1] J. Gubbi, R. Buyya, S. Marusic, and M. Palaniswami, "Internet of things (IoT): A vision, architectural elements, and future directions," *Future generation computer systems*, vol. 29, no. 7, pp. 1645–1660, 2013.

[2] S. Yinbiao, K. Lee, P. Lanctot, F. Jianbin, H. Hao, B. Chow, and J. Desbenoit, "Internet of things: wireless sensor networks," *White Paper, Intl. Electrotechnical Commission, http://www. iec. ch*, 2014.

[3] Y.-C. Wang and G.-W. Chen, "Efficient data gathering and estimation for metropolitan air quality monitoring by using vehicular sensor networks," *IEEE Trans. Veh. Technol.*, 2017.

[4] G. Zhao, "Wireless sensor networks for industrial process monitoring and control: A survey," *Network Protocols and Algorithms*, vol. 3, no. 1, pp. 46–63, 2011.

[5] D. Malan, T. Fulford-Jones, M. Welsh, and S. Moulton, "Codeblue: An ad hoc sensor network infrastructure for emergency medical care," in *Proc. MobiSys. Wksp. Applications of Mobile Embedded Systems (WAMES)*. Boston, MA, 2004, pp. 12–14.

[6] J. Jin, J. Gubbi, S. Marusic, and M. Palaniswami, "An information framework for creating a smart city through Internet of Things," *IEEE Internet of Things Jour.*, vol. 1, no. 2, pp. 112–121, 2014.

[7] G. Quer, R. Masiero, G. Pillonetto, M. Rossi, and M. Zorzi, "Sensing, compression, and recovery for WSNs: Sparse signal modeling and monitoring framework," *IEEE Trans. Wireless Commun.*, vol. 11, no. 10, pp. 3447–3461, 2012.

[8] S. Hwang, R. Ran, J. Yang, and D. K. Kim, "Multivariated Bayesian compressive sensing in wireless sensor networks," *IEEE Sensors Jour.*, vol. 16, no. 7, pp. 2196–2206, 2015.

[9] S. De and R. Singhal, "Toward uninterrupted operation of wireless sensor networks," *IEEE Computer*, vol. 45, no. 9, pp. 24–30, 2012.

[10] R. C. Shah, S. Roy, S. Jain, and W. Brunette, "Data MULEs: Modeling a three-tier architecture for sparse sensor networks," in *Proc. IEEE Intl. Wksp. Sensor Network Protocols and Applications*. Anchorage, AK, USA, 2003, pp. 30–41.

[11] Q. Ling and Z. Tian, "Decentralized sparse signal recovery for compressive sleeping wireless sensor networks," *IEEE Trans. Signal Process.*, vol. 58, no. 7, pp. 3816–3827, 2010.

[12] T. Xue, X. Dong, and Y. Shi, "Multiple access and data reconstruction in wireless sensor networks based on compressed sensing," *IEEE Trans. Wireless Commun.*, vol. 12, no. 7, pp. 3399–3411, 2013.

[13] Y. Chen and Q. Zhao, "On the lifetime of wireless sensor networks," *IEEE Commun. Lett.*, vol. 9, no. 11, pp. 976–978, 2005.

[14] S. Joshi and S. Boyd, "Sensor selection via convex optimization," *IEEE Trans. Signal Process.*, vol. 57, no. 2, pp. 451–462, 2009.

[15] M. Elad, "Optimized projections for compressed sensing," *IEEE Trans. Signal Process.*, vol. 55, no. 12, pp. 5695–5702, 2007.

[16] S. P. Chepuri and G. Leus, "Sparsity-promoting sensor selection for non-linear measurement models," *IEEE Trans. Signal Process.*, vol. 63, no. 3, pp. 684–698, 2015.

[17] W. Chen and I. J. Wassell, "Compressive sleeping wireless sensor networks with active node selection," in *Proc. IEEE Global Communications Conf. (GLOBECOM)*. Austin, TX, USA, 2014, pp. 7–12.

[18] ——, "Optimized node selection for compressive sleeping wireless sensor networks," *IEEE Trans. Veh. Technol.*, vol. 65, no. 2, pp. 827–836, 2016.

[19] R. Rieger and J. T. Taylor, "An adaptive sampling system for sensor nodes in body area networks," *IEEE Trans. Neural Sys. and Rehab. Engg.*, vol. 17, no. 2, pp. 183–189, 2009.

[20] A. Jain and E. Y. Chang, "Adaptive sampling for sensor networks," in *Proc. ACM Intl. Wksp. Data management for sensor networks: in conjunction with VLDB*. Toronto, Canada, 2004, pp. 10–16.

[21] A. D. Marbini and L. E. Sacks, "Adaptive sampling mechanisms in sensor networks," in *Proc. London Commun. Symp.*, vol. 174. London, UK, 2003.

[22] C. R. Rao, "The use and interpretation of principal component analysis in applied research," *Sankhyā: The Indian Jour. of Statistics, Series A*, pp. 329–358, 1964.

[23] D. L. Donoho, "Compressed sensing," *IEEE Trans. Inf. Theory*, vol. 52, no. 4, pp. 1289–1306, 2006.

[24] J. Hao, B. Zhang, Z. Jiao, and S. Mao, "Adaptive compressive sensing based sample scheduling mechanism for wireless sensor networks," *Pervasive and Mobile Computing*, vol. 22, pp. 113–125, 2015.

[25] S. S. Chen, D. L. Donoho, and M. A. Saunders, "Atomic decomposition by basis pursuit," *SIAM review*, vol. 43, no. 1, pp. 129–159, 2001.

[26] R. Tibshirani, "Regression Shrinkage and Selection via the LASSO," *Jour. of the Royal Statistical Society. Series B (Methodological)*, pp. 267–288, 1996.

[27] I. F. Gorodnitsky and B. D. Rao, "Sparse signal reconstruction from limited data using FOCUSS: A re-weighted minimum norm algorithm," *IEEE Trans. Signal Process.*, vol. 45, no. 3, pp. 600–616, Mar. 1997.

[28] S. G. Mallat and Z. Zhang, "Matching pursuits with time-frequency dictionaries," *IEEE Trans. Signal Process.*, vol. 41, no. 12, pp. 3397–3415, Dec. 1993.

[29] D. P. Wipf and B. D. Rao, "Sparse Bayesian learning for basis selection," *IEEE Trans. Signal Process.*, vol. 52, no. 8, pp. 2153–2164, Aug. 2004.

[30] R. Prasad, C. R. Murthy, and B. D. Rao, "Joint channel estimation and data detection in MIMO-OFDM systems: A sparse Bayesian learning approach," *IEEE Trans. Signal Process.*, vol. 63, no. 20, pp. 5369–5382, Oct. 2015.

[31] Z. Zhang, T.-P. Jung, S. Makeig, Z. Pi, and B. D. Rao, "Spatiotemporal sparse Bayesian learning with applications to compressed sensing of multichannel physiological signals," *IEEE Trans. Neural Sys. and Rehab. Engg.*, vol. 22, no. 6, pp. 1186–1197, Nov. 2014.

[32] V. Gupta, A. Mishra, S. Dwivedi, and A. K. Jagannatham, "SBL-based joint target imaging and Doppler frequency estimation in monostatic MIMO radar systems," in *Proc. IEEE Intl. Conf. Acoustics, Speech and Signal Processing (ICASSP)*. Shanghai, China, Mar. 2016, pp. 3011–3015.

[33] G. Quer, R. Masiero, D. Munaretto, M. Rossi, J. Widmer, and M. Zorzi, "On the interplay between routing and signal representation for compressive sensing in wireless sensor networks," in *IEEE Information Theory and Applications Workshop*, 2009, pp. 206–215.

[34] R. Masiero, G. Quer, D. Munaretto, M. Rossi, J. Widmer, and M. Zorzi, "Data acquisition through joint compressive sensing and principal component analysis," in *Proc. IEEE Global Telecommunications Conf.* Honolulu, HI, USA, 2009, pp. 1–6.

[35] A. Papoulis and S. U. Pillai, *Probability, random variables, and stochastic processes*. Tata McGraw-Hill Education, 2002.

[36] H. L. Van Trees, *Detection, estimation, and modulation theory*. John Wiley & Sons, 2004.

[37] K. B. Petersen, M. S. Pedersen *et al.*, "The matrix cookbook," *Technical University of Denmark*, vol. 7, p. 15, 2008.

[38] A. Nayebi-Astaneh, N. Pariz, and M.-b. Naghibi-Sistani, "Adaptive node scheduling under accuracy constraint for wireless sensor nodes with multiple bearings-only sensing units," *IEEE Trans. Aerosp. and Electron. Sys.*, vol. 51, no. 2, pp. 1547–1557, 2015.

[39] S. Boyd and L. Vandenberghe, *Convex optimization*. Cambridge university press, 2004.

[40] Z. Fei, B. Li, S. Yang, C. Xing, H. Chen, and L. Hanzo, "A survey of multi-objective optimization in wireless sensor networks: metrics, algorithms, and Open Problems," *IEEE Commun. Surveys and Tutorials*, vol. 19, no. 1, pp. 550–586, 2017.

[41] I. CVX Research, "CVX: Matlab software for disciplined convex programming, version 2.0," http://cvxr.com/cvx, Aug. 2012.

[42] J. V. Zidek, W. Sun, and N. D. Le, "Designing and integrating composite networks for monitoring multivariate Gaussian pollution fields," *Jour. of the Royal Statistical Society: Series C (Applied Statistics)*, vol. 49, no. 1, pp. 63–79, 2000.

[43] R. Prasad, B. N. Bharath, and C. R. Murthy, "Joint data detection and dominant singular mode estimation in time varying reciprocal mimo systems," in *Proc. IEEE Intl. Conf. Acoustics, Speech and Signal Processing (ICASSP)*. Prague, Czech Republic, 2011, pp. 3240–3243.

[44] M. Leinonen, M. Codreanu, and M. Juntti, "Sequential compressed sensing with progressive signal reconstruction in wireless sensor networks," *IEEE Trans. Wireless Commun.*, vol. 14, no. 3, pp. 1622–1635, 2015.

[45] D. Hooper, J. Coughlan, and M. Mullen, "Structural equation modelling: Guidelines for determining model fit," *The Electronic Jour. Business Research Methods*, vol. 6, pp. 53–60, 2008.

[46] Y. Zhang, "On extending some primal–dual interior-point algorithms from linear programming to semidefinite programming," *SIAM Jour. on Optimization*, vol. 8, no. 2, pp. 365–386, 1998.

[47] P. Bodik, W. Hong, C. Guestrin, S. Madden, M. Paskin, and R. Thibaux, "Intel lab data," *Online dataset*, 2004.

Vini Gupta received the B.Tech. degree in Electronics and Communication Engineering from Indira Gandhi Institute of Technology, Guru Gobind Singh Indraprastha University, New Delhi, India, in 2013 and the M.Tech. degree in Signal Processing and Communication from the Department of Electrical Engineering, IIT Kanpur, Uttar Pradesh, India, in 2016. She worked in Tata Consultancy Services Limited, New Delhi, as an Assistant System Engineer, from 2013 to 2014. She is currently working toward the Ph.D. degree in the Department of Electrical Engineering, IIT Delhi, New Delhi, India. Her research interests include design of energy efficient centralized and distributed sensing framework for wireless sensor networks-based IoT applications, sparse signal processing, application of Bayesian learning in wireless sensor networks, devise of trade-off optimization schemes in sensor networks, estimation and detection theory, radar signal processing. She is a recipient of TCS RSP Fellowship (2016-present).

Swades De (S'02-M'04-SM'14) received his B.Tech. degree in Radiophysics and Electronics from the University of Calcutta in 1993, the M.Tech. degree in Optoelectronics and Optical communication from IIT Delhi in 1998, and the Ph.D. degree in Electrical Engineering from the State University of New York at Buffalo in 2004.

Dr. De is currently a Professor with the Department of Electrical Engineering, IIT Delhi. Before moving to IIT Delhi in 2007, he was a Tenure-Track Assistant Professor with the Department of ECE, New Jersey Institute of Technology, Newark, NJ, USA, from 20042007. He worked as an ERCIM Post-doctoral Researcher at ISTI-CNR, Pisa, Italy (2004), and has nearly five years of industry experience in India on telecom hardware and software development, from 19931997, 1999. His research interests are broadly in communication networks, with emphasis on performance modeling and analysis. Current directions include energy harvesting sensor networks, broadband wireless access and routing, cognitive/white-space access networks, smart grid networks, and IoT communications. Dr. De currently serves as a Senior Editor of IEEE COMMUNICATIONS LETTERS, and an Associate Editor of IEEE TRANSACTIONS ON VEHICULAR TECHNOLOGY, IEEE WIRELESS COMMUNICATIONS LETTERS, IEEE NETWORKING LETTERS, and IETE Technical Review Journal.